Please cite this article in press as: Chen et al., Enhanced Fructose Utilization Mediated by *SLC2A5* Is a Unique Metabolic Feature of Acute Myeloid Leukemia with Therapeutic Potential, Cancer Cell (2016), http://dx.doi.org/10.1016/j.ccell.2016.09.006

Enhanced Fructose Utilization Mediated by *SLC2A5* Is a Unique Metabolic Feature of Acute Myeloid Leukemia with Therapeutic Potential

Wen-Lian Chen,[1,2,3,5] Yue-Ying Wang,[1,5] Aihua Zhao,[2,5] Li Xia,[1] Guoxiang Xie,[2,3] Mingming Su,[2,3] Linjing Zhao,[3] Jiajian Liu,[2] Chun Qu,[2] Runmin Wei,[3] Cynthia Rajani,[3] Yan Ni,[2,3] Zhen Cheng,[4] Zhu Chen,[1] Sai-Juan Chen,[1,*] and Wei Jia[2,3,6,*]

[1]State Key Laboratory of Medical Genomics, Department of Hematology, Shanghai Institute of Hematology, Rui Jin Hospital Affiliated with Shanghai Jiao Tong University School of Medicine, Shanghai 200025, China
[2]Center for Translational Medicine, Shanghai Jiao Tong University Affiliated Sixth People's Hospital, Shanghai 200233, China
[3]University of Hawaii Cancer Center, Honolulu, HI 96813, USA
[4]Molecular Imaging Program at Stanford, Department of Radiology and Bio-X Program, Canary Center at Stanford for Cancer Early Detection, School of Medicine, Stanford University, Stanford, CA 94305, USA
[5]Co-first author
[6]Lead Contact
*Correspondence: sjchen@stn.sh.cn (S.-J.C.), wjia@cc.hawaii.edu (W.J.)
http://dx.doi.org/10.1016/j.ccell.2016.09.006

SUMMARY

Rapidly proliferating leukemic progenitor cells consume substantial glucose, which may lead to glucose insufficiency in bone marrow. We show that acute myeloid leukemia (AML) cells are prone to fructose utilization with an upregulated fructose transporter GLUT5, which compensates for glucose deficiency. Notably, AML patients with upregulated transcription of the GLUT5-encoding gene *SLC2A5* or increased fructose utilization have poor outcomes. Pharmacological blockage of fructose uptake ameliorates leukemic phenotypes and potentiates the cytotoxicity of the antileukemic agent, Ara-C. In conclusion, this study highlights enhanced fructose utilization as a metabolic feature of AML and a potential therapeutic target.

INTRODUCTION

Acute myeloid leukemia (AML) is a heterogeneous disorder of hematopoietic stem cells characterized by uncontrolled proliferation of aberrant clones of myeloid progenitor cells with impaired differentiation and by suppressed production of healthy hematopoietic cells. The pathogenesis of AML involves two types of gene mutations, class I mutations that induce cellular proliferation and class II mutations that compromise normal differentiation (Ferrara and Schiffer, 2013). In addition, a third class of genes encoding epigenetic modifiers, such as *DNMT3A*, *IDH1*, *IDH2*, and *TET2*, are found to play a major role in leukemogenesis (Ferrara and Schiffer, 2013). Recent studies showed that aberrant metabolism was also critically involved in the pathogenesis and progression of AML (Chen et al., 2014; Losman et al., 2013).

Conventional drug therapy for AML usually includes a cell-cycle inhibitor, arabinofuranosyl cytidine (Ara-C), which targets cells in the S or DNA synthesis phase, and a topoisomerase II inhibitor, such as an anthracycline derivative (usually daunorubicin). The anthracyclines also target dividing cells preferentially by inhibiting DNA transcription/replication but are classified as cell-cycle-independent drugs (Martincic and Hande, 2005). Due to the diverse genetic and epigenetic abnormalities of individual patients, treatment efficacy and prognosis may vary significantly and there is no single treatment to cure AML patients of different molecular subtypes (Ferrara and Schiffer, 2013; Patel et al., 2012). On the other hand, the downstream

Significance

Glucose, a well-known carbon source, has been extensively studied in various cancers. However, little is known about the role of fructose, the second most abundant blood sugar, in cancers including AML. This study shows that AML cells predominantly use fructose as an important glucose alternative to promote cell proliferation. Enhanced fructose utilization aggravates the leukemic phenotypes of AML cells thus causing poor outcomes in patients. This unique metabolic feature may create an important biological target since most normal cells including normal monocytes do not use fructose as the main metabolic fuel. Small-molecule chemical agents or antibodies that can inhibit or block fructose uptake will selectively inhibit AML cell growth and synergize with antileukemic drugs.

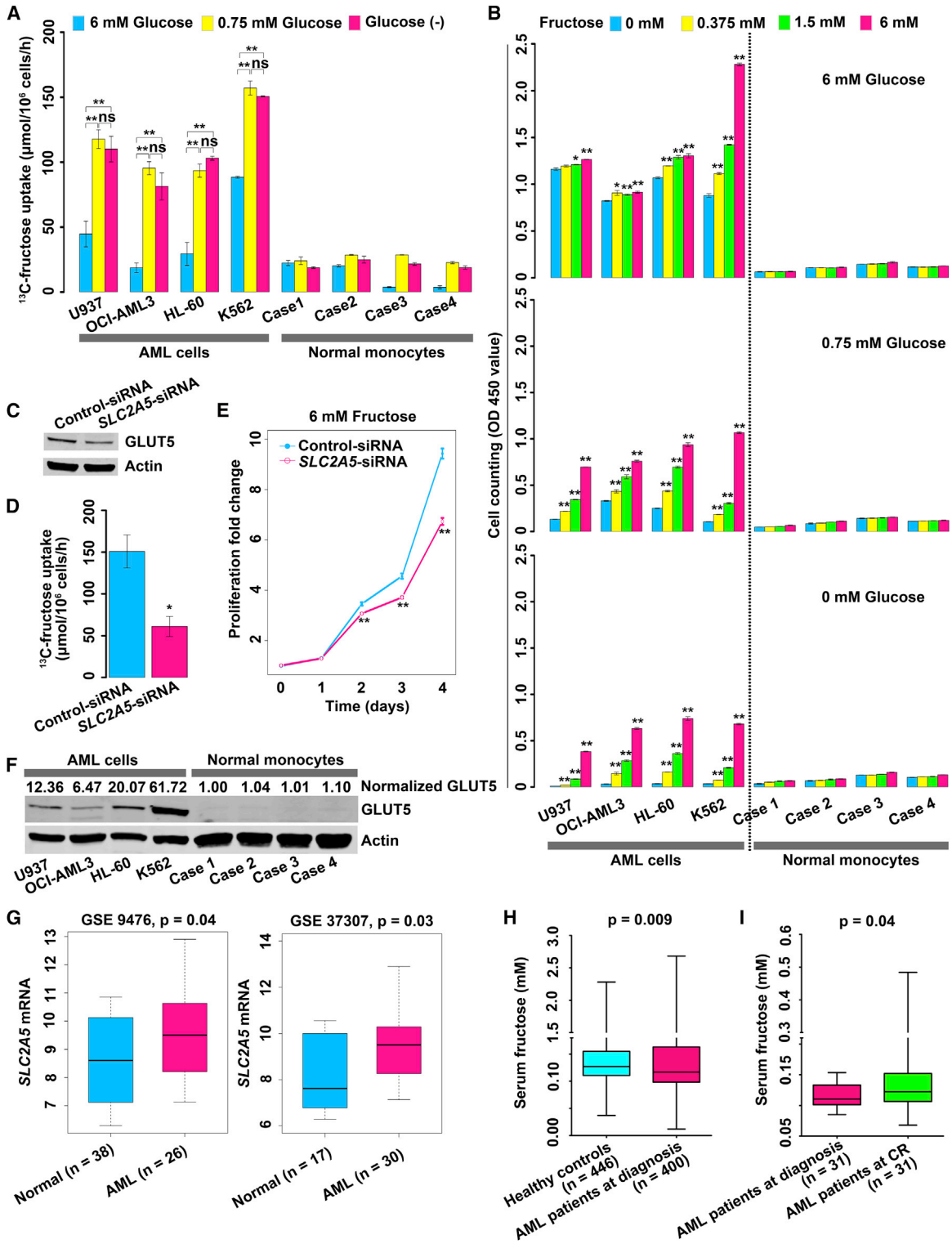

Figure 1. Fructose Utilization by AML Cells

(A) ^{13}C-Fructose uptake by AML cells and normal monocytes. ns, not significant.

(B) Fructose-induced proliferation of AML cells and normal monocytes under the conditions of different glucose levels. Cells were grown in the media for 72 hr. For each glucose condition, p values were obtained by comparison with the cell proliferation in 0 mM fructose.

(C) Western blot showing GLUT5 knockdown in K562 cells by small interfering RNA targeting *SLC2A5*.

(D) Uptake of ^{13}C-fructose by K562 cells with or without *SLC2A5* inhibition.

(legend continued on next page)

metabolic alterations involve a more limited number of core pathways that show relatively low diversity (Cairns et al., 2011; Jang et al., 2013). For example, increased glycolysis (Warburg effect) is a common metabolic feature in various cancer cells, and it has been under extensive investigation as a therapeutic target for cancer.

A good strategy to inhibit accelerated glycolysis is to block excessive metabolic fuel uptake. Inhibition of glycolysis using a glucose analog, 2-deoxyglucose (2-DG), has already been shown to re-sensitize acute lymphoblastic leukemia (ALL) cells to prednisolone therapy (Hulleman et al., 2009). The combination of 2-DG and an MCL1 anti-apoptotic protein inhibitor has proved to be synergistic in overcoming prednisolone resistance in ALL cells (Aries et al., 2013). Our recent study of AML cell lines revealed enhanced expression of genes relating to both glycolysis and the tricarboxylic acid (TCA) cycle (Chen et al., 2014). The same study also identified a panel of six elevated serum metabolites related to glycolysis and the TCA cycle in a cohort of 223 de novo cytogenetically normal AML patients, which predicted poor survival outcomes independent of cytogenetic risk. Reducing glycolysis that is upstream of the TCA cycle may thus prove beneficial in AML.

Normal, non-proliferating cells switch to glycolysis only under hypoxic conditions (Lum et al., 2007). Hypoxia promotes the switch to glycolytic metabolism via the hypoxia-inducible factor-1 pathway, and progression of AML has been linked to the expansion of hypoxia in the subendosteal bone marrow niche relative to normal bone marrow (Tabe and Konopleva, 2014). It has been reported that AML cells display a highly active glycolytic metabolism (Herst et al., 2011). Such an increase in glycolytic flux in AML cells would accelerate glucose consumption and lead to glucose insufficiency in the bone marrow. In fact, significantly lower glucose levels are found in leukemic bone marrow relative to peripheral blood (Tiziani et al., 2013). Thus, a flexible metabolic program is required for AML cells to accommodate a low-glucose environment. Fructose is the second most abundant blood sugar in humans with a physiologically normal range of 0.5–1.0 mM (Barone et al., 2009; Liu et al., 2010). Based on these observations, we hypothesized that AML cells will show increased expression of the fructose transporter, GLUT5, and exhibit enhanced fructose utilization relative to normal cells especially under low-glucose conditions.

RESULTS

AML Cells Exhibited Increased Fructose Utilization under Low-Glucose Conditions

For the first set of experiments we hypothesized that AML cells would switch to fructose utilization especially in the absence or low level of glucose. In order to assess fructose utilization in AML cells, two parameters were selected, fructose uptake and fructose-induced cell proliferation. Four AML cell lines with distinct genetic backgrounds along with four different batches of normal monocytes as controls were employed for both assays (Table S1). All of the cells were able to import ^{13}C-fructose (Figure 1A). However, AML cells displayed a higher fructose transport rate than normal monocytes under conditions of glucose deficiency (0 or 0.75 mM). Fructose uptake was significantly increased in the leukemic cells under glucose deficiency (0 or 0.75 mM) compared with glucose sufficiency (6 mM) ($p < 0.01$).

The next objective was to determine if fructose uptake led to enhanced proliferation of AML cells under glucose-deficient conditions. The results showed that AML cells exhibited a significant increase ($p < 0.01$) in proliferation induced by fructose under conditions of low glucose or glucose deprivation, indicating that fructose was an important fuel source for AML cells when glucose was limited (Figure 1B). In contrast, in the presence of fructose, normal monocytes displayed little or no increases in proliferation under any of the tested glucose conditions, indicating that normal monocytes showed significantly lower fructose utilization compared with AML cells (Figure 1B). We concluded from these studies that AML cells not only readily utilize fructose as a metabolic fuel for survival but also that their ability to proliferate is actually enhanced by increased fructose under glucose-limiting conditions, whereas normal monocytes hardly rely on fructose for growth.

GLUT5 Mediated Fructose Uptake and Had Increased Expression in AML Cells

Having established that AML cells readily utilize fructose, the next step was to identify the sugar transporter that was being used for fructose uptake. GLUT5, encoded by the *SLC2A5* gene, has been reported to be the main transporter for fructose with high selectivity in various cells (Burant et al., 1992; Zhao and Keating, 2007). Thus, we hypothesized that the sugar transporter involved in AML cell fructose utilization was in fact, GLUT5. We tested this hypothesis by knocking down the *SLC2A5* gene in K562 cells using an RNAi technique (Figure 1C). The results showed that both ^{13}C-fructose uptake and fructose-induced proliferation were suppressed (Figures 1D and 1E). *SLC2A5* gene silencing did not affect glucose uptake and glucose-induced proliferation in K562 cells (Figures S1A and S1B), indicating the selectivity of this transporter for fructose. These data demonstrated that GLUT5 mediated the fructose uptake in AML cells.

Increased GLUT5 expression was observed in all four of the AML cell lines compared with normal monocytes (Figure 1F).

(E) Fructose-induced proliferation of K562 cells with or without *SLC2A5* inhibition.
(F) GLUT5 expression between AML cells and normal monocytes. Relative GLUT5 expression was computed by dividing the value of GLUT5 signal intensity by the value of actin signal intensity. Normalized GLUT5 was obtained by normalizing each relative GLUT5 expression to the mean of relative GLUT5 expression of four cases of normal monocytes.
(G) The expression of GLTU5-encoding gene *SLC2A5* between normal hematopoietic cells of healthy controls and AML blast cells of patients. The data were obtained from a public microarray database.
(H) Serum fructose concentration comparison between healthy controls and AML patients.
(I) Serum fructose concentration of paired samples from 31 AML patients at diagnosis and at complete remission (CR).
Error bars represent mean ± SEM. *$p < 0.05$, **$p < 0.01$ (Student's t test). See also Figure S1 and Tables S1 and S2.

The next question was whether GLUT5 or its encoding gene *SLC2A5* was also upregulated in primary AML blast cells from de novo AML patients. We analyzed gene expression patterns of the major sugar transporter genes in primary AML blast cells using previously published microarray datasets (Stirewalt et al., 2008, 2012) and determined that *SLC2A5* gene expression was significantly increased in blast cells compared with normal hematopoietic cells, indicating the increased fructose uptake capability of patient-derived AML cells (Figure 1G). In contrast, for the well-known glucose transporter genes, *SLC2A1*, *SLC2A2*, and *SLC2A4*, there were no significant differences between primary AML cells and normal hematopoietic cells, while *SLC2A3* showed significant reduction in primary AML cells (Figure S1C). Subsequently, we explored the possible mechanism for upregulating *SLC2A5* in primary AML blast cells. We analyzed the datasets including GEO: GSE1159, GSE425, and The Cancer Genome Atlas data (Bullinger et al., 2004; Valk et al., 2004) and found that *SLC2A5* expression was positively correlated to *AML1-ETO*, *NPM1* mutations, and *RUNX1* mutations, whereas it was negatively linked to *PML-RARA* and *CEBPA* biallelic mutations, indicating that overexpression of *SLC2A5* may be secondary to these gene events (Table S2).

Based on above observations, we hypothesized that increased expression of *SLC2A5* in primary AML blast cells would accelerate fructose utilization thus resulting in reduced circulating fructose in peripheral blood. To test this hypothesis, serum samples from healthy controls (n = 446) and AML patients (n = 400) were analyzed using gas chromatograph-time-of-flight mass spectrometry (GC-TOFMS). To avoid the well-known confounding factors influencing circulating fructose level, including hepatic function, diet, and therapy, we executed the following strategies. First, we reviewed the key parameters of hepatic function including serum alanine aminotransferase and aspartate aminotransferase in all enrolled subjects and confirmed that there was no significant difference in hepatic function between AML patients and healthy controls (Chen et al., 2014). Second, all serum samples were collected from 12-hr fasting peripheral blood to minimize dietary impact. Third, all AML serum samples were obtained from patients at diagnosis without any therapeutic interventions. Data from GC-TOFMS showed reduced serum fructose concentrations in AML patients relative to controls (Figure 1H), suggesting elevated fructose utilization of leukemic blast cells in these patients. Hypothesizing that AML blast cells were responsible for the reduction of serum fructose, when these neoplastic cells were eliminated by chemotherapy, the serum fructose level would be expected to increase. To test this hypothesis, we analyzed paired serum samples from AML patients (n = 31) at diagnosis and at complete remission (CR) and found that serum fructose was significantly raised in the cases at CR compared with those at diagnosis ($p = 0.04$, Figure 1I), supporting our hypothesis that AML blast cells contributed to the decrease of serum fructose.

In summary, these results provided convincing evidence that an increase in the sugar transporter GLUT5 encoded by *SLC2A5*, was responsible for the increased uptake and utilization of fructose in our test set of AML cell lines and also in the primary leukemic cells of AML patients.

High Expression of *SLC2A5* and Enhanced Fructose Utilization Were Associated with Poor Outcomes in AML Patients

Based on the above observations of increased fructose utilization and upregulated fructose transporter GLUT5 and its encoding gene *SLC2A5* in AML cells, we asked if there was an association between the modified *SLC2A5* expression/fructose utilization and the therapeutic outcomes of AML patients. We analyzed the relevance of *SLC2A5* expression to the survival of AML patients in five previously published gene expression datasets (Bullinger et al., 2004; Metzeler et al., 2008; Valk et al., 2004). Among those cases, patients with intermediate-risk AML were selected for analysis due to the relatively low heterogeneity in this subgroup. The patients of each set were divided into two groups: those with above-median *SLC2A5* expression and those with below-median *SLC2A5* expression. Above-median *SLC2A5* expression was associated with inferior overall survival, and a formal meta-analysis of all five datasets indicated an overall hazard ratio of 1.49 (95% confidence interval [CI]: 1.41–1.57) in a univariate Cox model and 1.48 (95% CI, 1.34–1.62) in a multivariate Cox model after adjustment for clinical confounding factors including age, white blood cell count, and *FLT3*-ITD mutations (Figure 2A). To avoid the potential statistical bias, we used the mean instead of median value of *SLC2A5* expression as the cut-off point in each dataset. Above-mean *SLC2A5* expression was also closely linked to poor overall survival, and a formal meta-analysis of all five datasets demonstrated an overall hazard ratio of 1.87 (95% CI, 1.24–2.50) in the Cox model (Figure S2A).

Subsequently, we analyzed the potential correlation between fructose utilization and therapeutic response in 262 de novo AML patients from data collected in a previous study (Chen et al., 2014). These patients were evenly divided into three groups based on their serum fructose concentrations: high, medium, and low fructose (Figure 2B), representing low, medium, and high fructose utilization, respectively. We found that the rate of treatment failure was increased and the CR rate was reduced when fructose utilization was elevated (Figure 2C), demonstrating that enhanced fructose utilization was associated with poor therapeutic response in AML patients. Of note, there was no significant difference in the overall survival and event-free survival among these three groups of AML patients (Figures S2B and S2C).

Enhanced Fructose Utilization Mediated by *SLC2A5* Exacerbated Leukemic Phenotypes

High *SLC2A5* expression and enhanced fructose utilization were closely associated with the poor outcomes of AML patients. In addition, downregulation of *SLC2A5* in K562 cells significantly suppressed fructose-induced colony formation (Figure S3A). Thus, we hypothesized that enhanced fructose utilization mediated by *SLC2A5* would result in a more malignant phenotype. We ectopically expressed *SLC2A5* in U937, K562, and OCI-AML3 cells (Figures 3A, S3B, and S3C) as they were typical representatives of AML with distinct genetic aberrations and risk status (Table S1). To determine the fructose concentration to be used for the in vitro study, we first investigated the level of this sugar in bone marrow from AML patients that hosted living primary AML blast cells. There

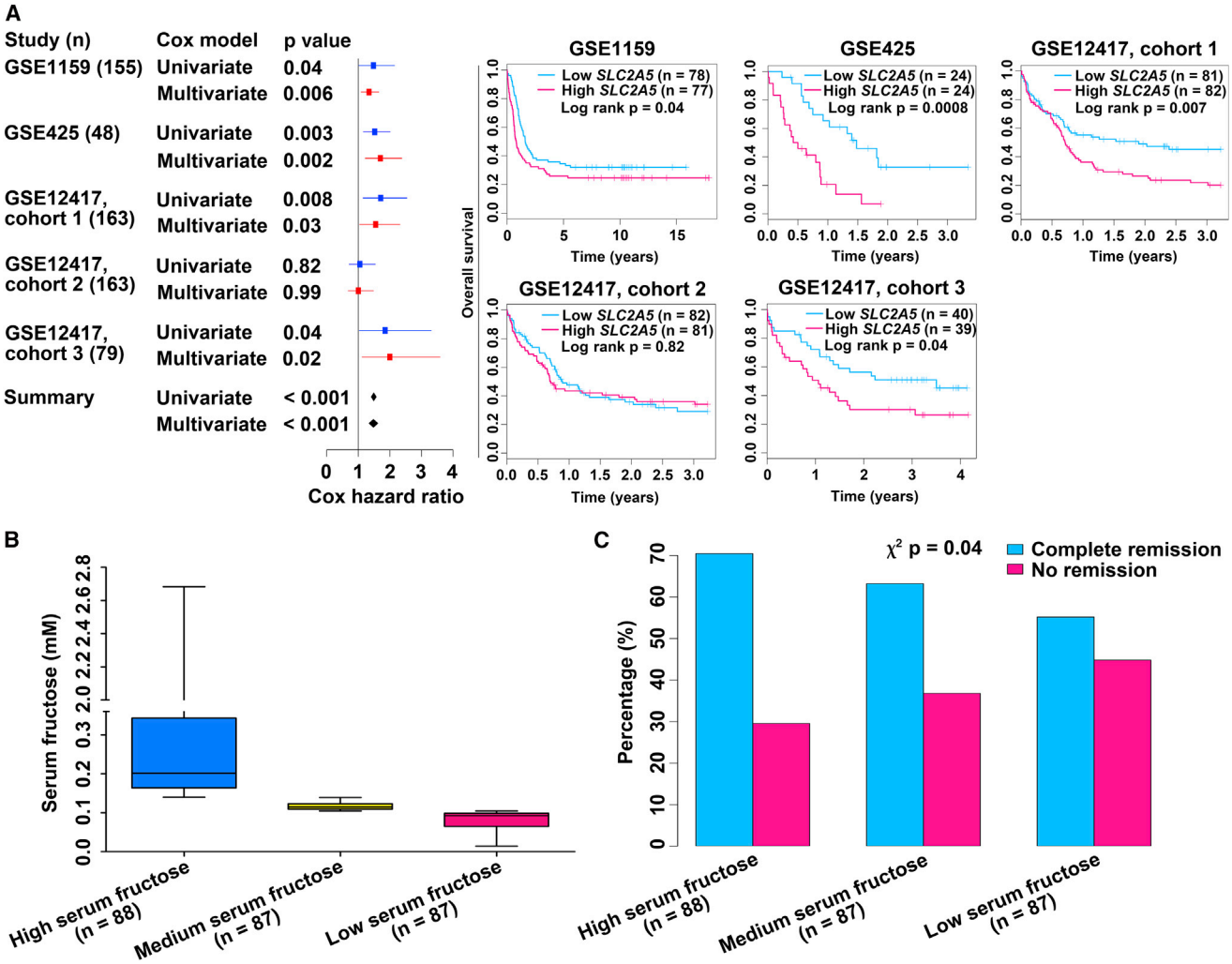

Figure 2. Prognostic Value of *SLC2A5* Expression Levels and Fructose Utilization Rates in AML Patients

(A) (Left) Meta-analysis of Cox hazard ratio of *SLC2A5* expression levels in five datasets containing patients with intermediate-risk AML. Solid horizontal lines denoted 95% confidence intervals; boxes denoted the relative influence of each set over the results; the diamonds indicate the summary 95% confidence interval. The continuous *SLC2A5* value was used in the analysis. (Right) Kaplan-Meier survival curves of five cohorts of patients in the left meta-analysis. Patients were separated into above-median (deep pink line) and below-median (deep sky blue line) of *SLC2A5* expression.

(B) AML patients were evenly divided into three groups according to the serum levels of fructose.

(C) The complete remission and no remission rates of three AML groups in (B).

See also Figure S2.

were only three AML patients who had paired bone marrow and peripheral blood samples in our previous metabolomic study, and the data showed that fructose concentration was elevated in bone marrow with a range of 0.71–4.74 mM compared with the serum levels ranging from 0.02 to 0.41 mM (Figure S3D). In addition, we assayed unpaired bone marrow (n = 7) and peripheral blood (n = 10) samples from patients with hematological malignancies and also found elevated fructose levels in bone marrow (p = 0.007, Table S3). Hence, we used 6 mM fructose, which was pathophysiologically relevant to AML, to perform the in vitro assays. Compared with the control cells (U937-MigR1, K562-MigR1, and OCI-AML3-MigR1), gene-modified cells (U937-*SLC2A5*, K562-*SLC2A5*, and OCI-AML3-*SLC2A5*) displayed increased ^{13}C-fructose uptake (Figures 3B, S3E, and S3F). Enforced *SLC2A5* expression also increased fructose-induced proliferation under distinct glucose conditions (Figures 3C–3E and S3G–S3L). These results indicated that enhanced fructose utilization mediated by *SLC2A5* conferred a proliferation advantage on AML cells even in the presence of glucose.

We then investigated the proliferation of transfected AML cells under low-fructose conditions (0.375 mM) in the absence of glucose and found that ectopic expression of *SLC2A5* accelerated the proliferation of K562 and OCI-AML3, whereas transfected U937 cells were unable to grow under such a fructose-limiting condition (Figures S3M–S3O).

The next question was whether enhanced fructose utilization influenced the malignancy of AML cells. To determine this, we

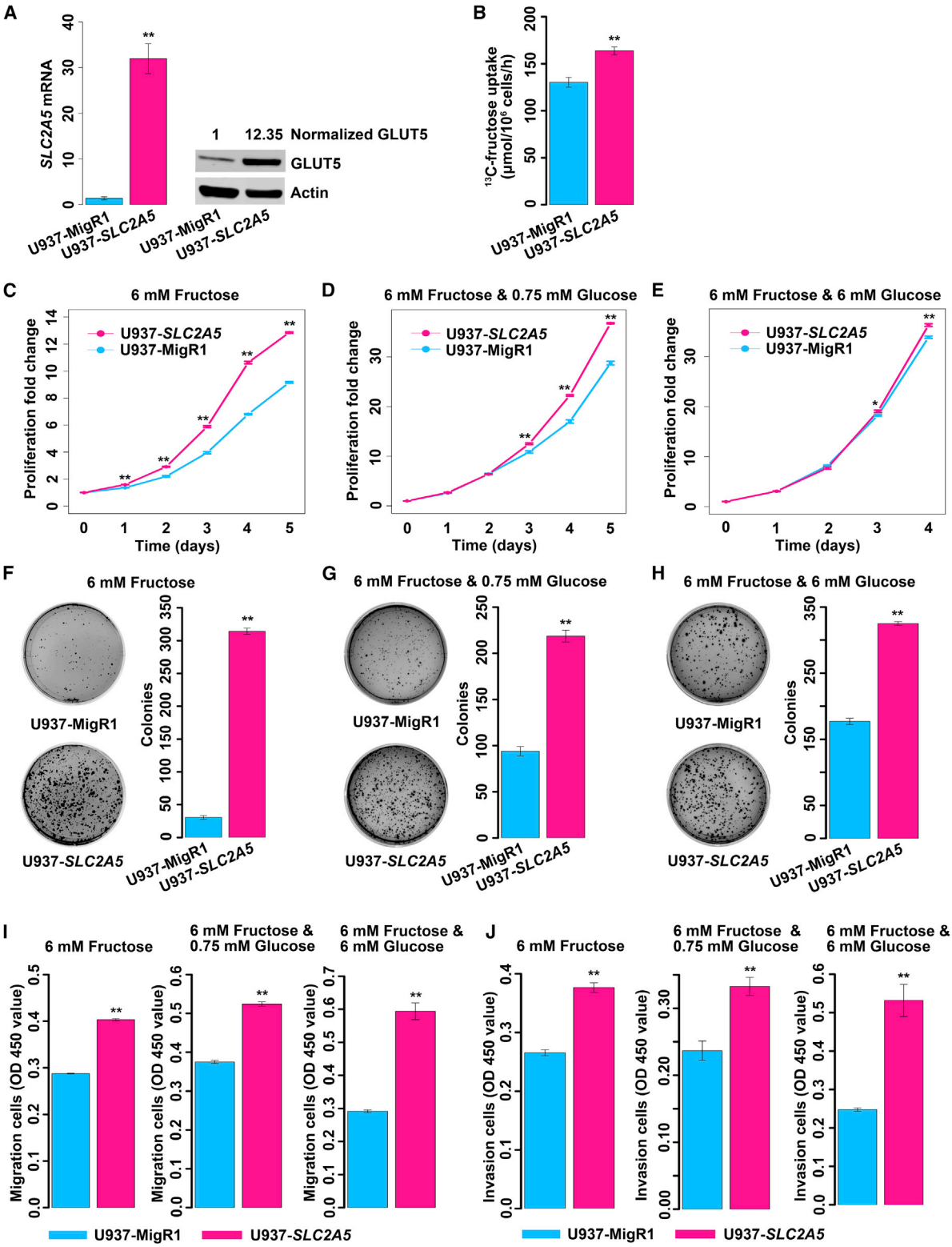

Figure 3. Enhanced Fructose Utilization Mediated by *SLC2A5* Exacerbates the Leukemic Phenotypes of AML Cells

(A) Measurement of the expression of *SLC2A5*/GLUT5 in U937 cells transfected with the control MigR1 retrovirus (U937-MigR1) or MigR1-*SLC2A5* retrovirus (U937-*SLC2A5*) by qPCR and western blot.

(B) Uptake of ^{13}C-labeled fructose by U937-MigR1 and U937-*SLC2A5* cells.

(C–E) Proliferation of U937-MigR1 and U937-*SLC2A5* cells in complete medium containing 6 mM fructose without glucose or with distinct levels of glucose.

(legend continued on next page)

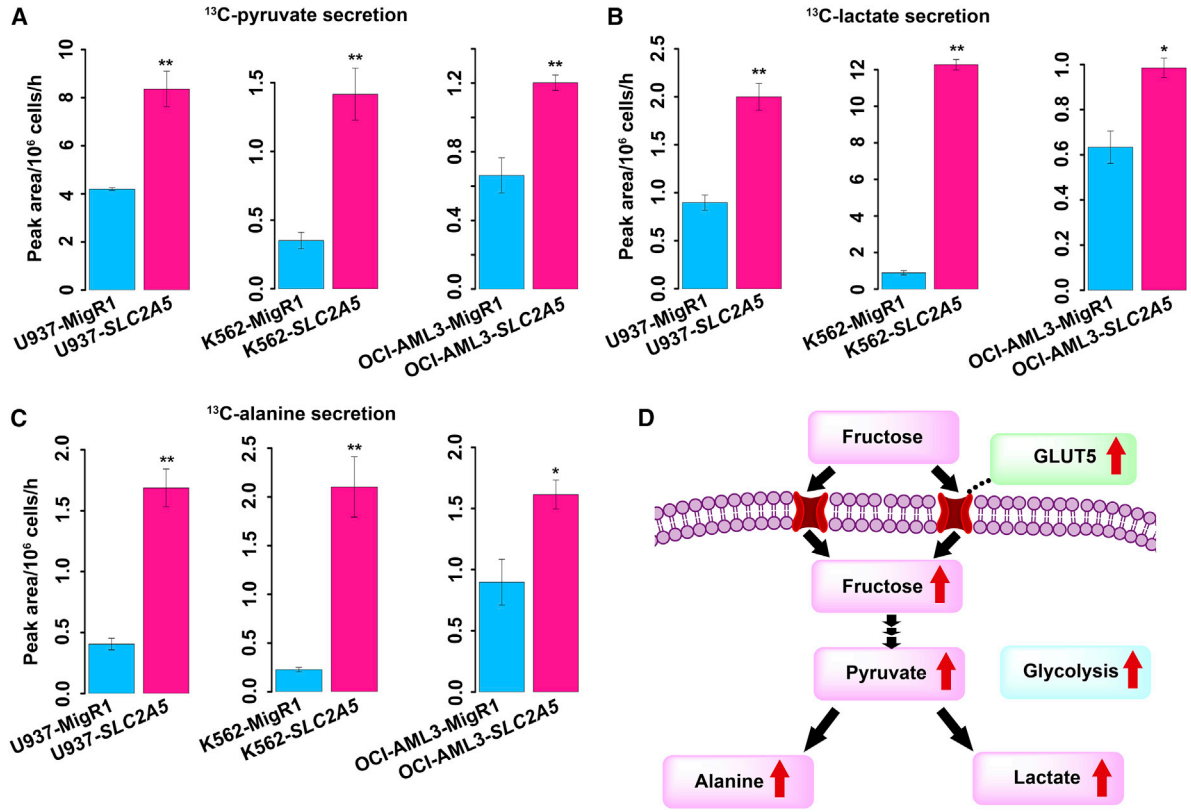

Figure 4. Enhanced Fructose Utilization Mediated by *SLC2A5* Activates Glycolytic Flux

(A) Secretion of ^{13}C-labeled pyruvate derived from ^{13}C-fructose tracer by AML control cells and AML cells with ectopic *SLC2A5*.

(B) Secretion of ^{13}C-labeled lactate derived from ^{13}C-fructose tracer by AML control cells and AML cells with ectopic *SLC2A5*.

(C) Secretion of ^{13}C-labeled alanine derived from ^{13}C-fructose tracer by AML control cells and AML cells with ectopic *SLC2A5*.

(D) Proposed metabolic scheme depicting increased glycolytic flux activated by enhanced fructose utilization mediated by *SLC2A5*.

Error bars represent mean ± SEM. *p < 0.05, **p < 0.01 (Student's t test).

assayed the influence of enhanced fructose utilization ability on colony formation in soft agar, a parameter positively associated with increased cancer cell malignancy (Zebisch et al., 2012). As depicted by the data in Figures 3F–3H and S4A–S4F, AML cells with ectopic *SLC2A5* fed with fructose exhibited increased colony growth relative to control cells under distinct glucose conditions. This indicated that enhanced fructose utilization mediated by *SLC2A5* exacerbated the malignant phenotype of AML cells, even in the presence of glucose.

Finally, we investigated whether enhanced fructose utilization was able to promote the capability of migration and invasion. As shown in Figures 3I, 3J, and S4G–S4J, enhanced fructose utilization mediated by *SLC2A5* significantly increased the migratory and invasive tendency of AML cells under reduced or normal glucose conditions, implying that enhanced fructose utilization causes a more aggressive phenotype regardless of glucose concentration.

Enhanced Fructose Utilization Mediated by *SLC2A5* Strongly Activated Glycolytic Flux

Logically, one would suppose that enhanced proliferation and enhanced fuel uptake in the form of fructose would cause increased glycolytic flux and result in increased amounts of metabolites from glycolysis. We performed a metabolic flux assay to establish whether an increased glycolytic flux was a possible explanation for the more aggressive tendency exhibited by AML cells. We compared the metabolic flux of ^{13}C-labeled fructose between non-transfected AML control cells and AML cells with ectopic *SLC2A5*. All cells were cultured in 6 mM ^{13}C-fructose for 96 hr and then the spent media were collected for analysis. AML cells with enhanced fructose utilization mediated by ectopic *SLC2A5* produced more ^{13}C-pyruvate, ^{13}C-lactate, and ^{13}C-alanine than the control cells (Figures 4A–4C). This indicated that enhanced fructose utilization in AML cells strongly activated glycolytic flux (Figure 4D).

(F–H) Colony formation of U937-MigR1 and U937-*SLC2A5* cells in soft agar fed with complete medium containing 6 mM fructose without glucose or with distinct levels of glucose. Cells were seeded at a density of 3,000/well (F), 2,000/well (G), or 1,000/well (H). Colonies were assayed at day 23 (F) or day 16 (G and H).

(I) Migration of U937-MigR1 and U937-*SLC2A5* cells fed with complete medium containing 6 mM fructose without glucose or with different levels of glucose.

(J) Invasion of U937-MigR1 and U937-*SLC2A5* cells fed with complete medium containing 6 mM fructose without glucose or with different levels of glucose.

Error bars represent mean ± SEM. *p < 0.05, **p < 0.01 (Student's t test).

See also Figures S3 and S4 and Table S3.

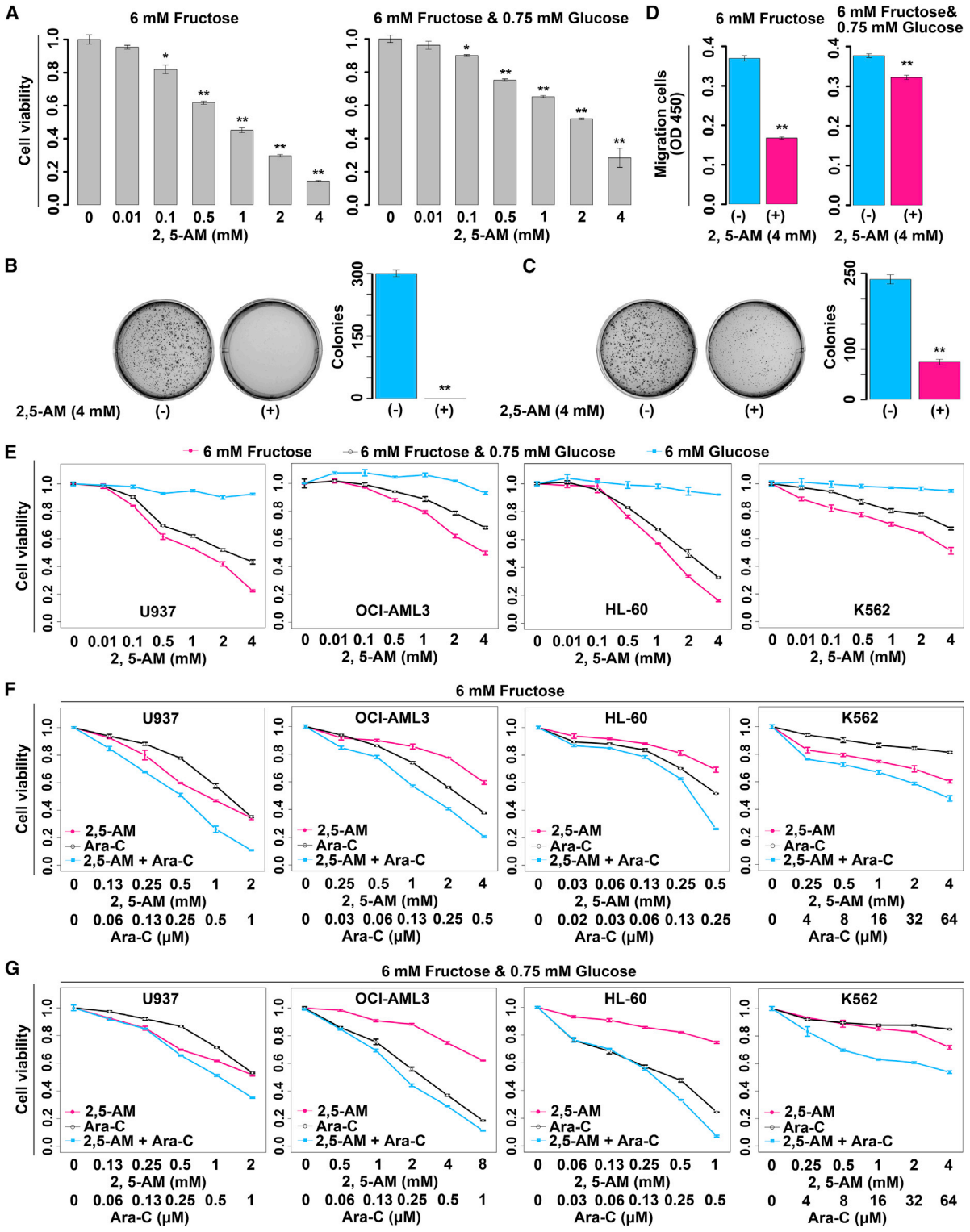

Figure 5. Response of AML Cells to Pharmacological Blockage of Fructose Utilization

(A) Suppressed proliferation of U937-*SLC2A5* cells treated with the fructose analog 2,5-AM. Two carbon source conditions, 6 mM fructose and 6 mM fructose plus 0.75 mM glucose, were tested. p Values were obtained by comparison with the proliferation of U937-*SLC2A5* cells in 0 mM 2,5-AM.

(B and C) The colony growth of U937-*SLC2A5* cells in soft agar under the condition of 6 mM fructose (B) or 6 mM fructose plus 0.75 mM glucose (C) with or without 2,5-AM treatment.

(D) Migration assay of U937-*SLC2A5* cells with or without 2,5-AM treatment in medium containing 6 mM fructose or 6 mM fructose plus 0.75 mM glucose.

(legend continued on next page)

Pharmacological Blockage of Fructose Utilization Alleviated Leukemic Phenotypes and Potentiated the Cytotoxicity of an Antileukemic Drug, Ara-C, In Vitro

Due to the causal relation between enhanced fructose utilization and exacerbation of leukemic phenotypes, we asked if inhibiting fructose utilization with a pharmacological agent would be able to alleviate the leukemic phenotypes. We used 2,5-anhydro-D-mannitol (2,5-AM), a fructose analog with high affinity for GLUT5 (Yang et al., 2002), to treat AML cells with enhanced fructose utilization mediated by ectopic *SLC2A5* expression. Data showed that 2,5-AM treatment significantly suppressed fructose-induced proliferation, colony growth, and migration in the absence of glucose or in the presence of low levels of glucose (Figures 5A–5D and S5A–S5H). The combination of the results supported the hypothesis that inhibition of fructose utilization decreases the malignant leukemic phenotypes of AML cells with enhanced fructose utilization.

Next, we investigated the efficacy of 2,5-AM on all of the four AML cell lines enrolled in this study. This drug suppressed fructose-induced cell proliferation in a dose-dependent manner in all AML cell lines under glucose-limiting conditions, whereas it had little influence on the glucose-induced cell proliferation (Figure 5E). Normal monocytes were also tested using 2,5-AM and there was negligible effect on glucose-induced cell growth (Figure S5I). Together, these results demonstrated a high specificity for the GLUT5 inhibitor, 2,5-AM, on inhibition of fructose utilization.

AML is usually treated with a combination of a cell-cycle-independent drug such as daunorubicin and a cell-cycle-specific inhibitor such as Ara-C (Martincic and Hande, 2005; Momparler, 2013). Because cancer therapy rarely involves administration of a single drug, we chose to replace daunorubicin with 2,5-AM and co-administer it with Ara-C to our four cell lines. Of note, a synergistic effect between 2,5-AM and Ara-C was observed in all AML cell lines grown in fructose without glucose or with low levels of glucose, demonstrating that 2,5-AM potentiated the cytotoxicity of the currently used AML drug, Ara-C (Figures 5F and 5G, Table S4). To summarize these results, 2,5-AM, a GLUT5 inhibitor was cytotoxic to AML cells, but not to normal monocytes, and also decreased the malignant phenotypes of AML cells with enhanced fructose utilization observed in these studies. The combination of 2,5-AM and Ara-C acts in a synergistic way to eradicate AML cells.

Fructose Utilization Was Enhanced in AML Mice and Pharmacological Blockage of This Metabolic Pathway Showed Therapeutic Potential

We performed a study using an AML mouse model driven by the fusion gene *AML1-ETO* and mutated *C-KIT* (Wang et al., 2011) to investigate the activity of fructose utilization and the therapeutic potential of pharmacological blockage of this metabolic pathway in vivo. It was reasonable to choose this mouse model because *SLC2A5* expression was positively associated with *AML1-ETO* in AML patients (Table S2), and patients with *AML1-ETO* and *C-KIT* mutations exhibited increased fructose utilization (Figure S6). Five mouse groups were enrolled, including a normal control group, AML mice treated with vehicle (vehicle group), AML mice treated with 2,5-AM (2,5-AM group), AML mice treated with Ara-C (Ara-C group), and AML mice treated with 2,5-AM and Ara-C (2,5-AM + Ara-C group). We assayed the parameters of these five groups of mice 17 days after leukemic cell transplantation (Table S5). Compared with normal controls, AML mice showed increased *SLC2A5* expression in bone marrow cells (Figure 6A). AML mice also exhibited reduced serum fructose levels (Figure 6B). These data indicated that fructose utilization was enhanced in AML mice. Administration of 2,5-AM significantly upregulated serum fructose concentrations in AML mice of the vehicle group ($p < 0.01$) and the 2,5-AM + Ara-C group ($p < 0.001$) (Figure 6B), indicating that fructose utilization in vivo was suppressed by this reagent. Inhibition of fructose utilization by 2,5-AM in AML mice significantly suppressed the growth of bone marrow and peripheral AML blast cells, and ameliorated splenomegaly (Figures 6C–6E). In addition, 2,5-AM administration improved the impaired peripheral blood cell counts as shown by the decrease in white blood cells ($p < 0.001$) and increase in red blood cells ($p = 0.01$), hemoglobin ($p = 0.01$), and platelets ($p = 0.04$) (Figures 6F–6I). Furthermore, the use of 2,5-AM prolonged the overall survival of AML mice ($p = 0.01$, Figure 6J). Of note, the combination of 2,5-AM and Ara-C showed an increased efficacy in alleviating leukemic phenotypes compared with 2,5-AM or Ara-C alone (Figures 6C, 6D, and 6F–6I). Moreover, the effect of 2,5-AM or Ara-C alone on overall survival of the AML mice was enhanced by the concurrent use of 2,5-AM and Ara-C ($p < 0.001$ and $p = 0.08$, respectively) (Figure 6J), demonstrating a synergistic antitumor effect between these two agents against AML.

DISCUSSION

Considerable attention has been paid to glycolysis due to its high activity in cancer cells and its close association with therapeutic resistance and clinical outcome (Zhao et al., 2013). Glycolysis has been found to be enhanced in AML and is linked to poor survival in patients partially via contribution to Ara-C resistance (Chen et al., 2014). Thus, drugs, such as 2-DG, aiming at interrupting glucose utilization in cancer cells may have potential for improvement of therapeutic outcome (Chen et al., 2014). Unfortunately, since normal cells also use glucose as their main metabolic fuel, inhibiting glucose utilization with 2-DG causes substantial adverse side effects, including hypoglycemia-like symptoms, gastrointestinal bleeding, hypotension, decreased respiratory frequency, as well as hematologic and biochemical toxicity (Raez et al., 2013; Vijayaraghavan et al., 2006). It is therefore important to fully understand the distinct metabolic features of fuel utilization for both AML and normal cells.

(E) Proliferation of AML cells treated with 2,5-AM. Three carbon resource conditions were tested.
(F and G) The synergistic effect between 2,5-AM + Ara-C in AML cells cultured in complete medium containing 6 mM fructose (F) or 6 mM fructose plus 0.75 mM glucose (G).
Error bars represent mean ± SEM. *$p < 0.05$, **$p < 0.01$ (Student's t test).
See also Figure S5 and Table S4.

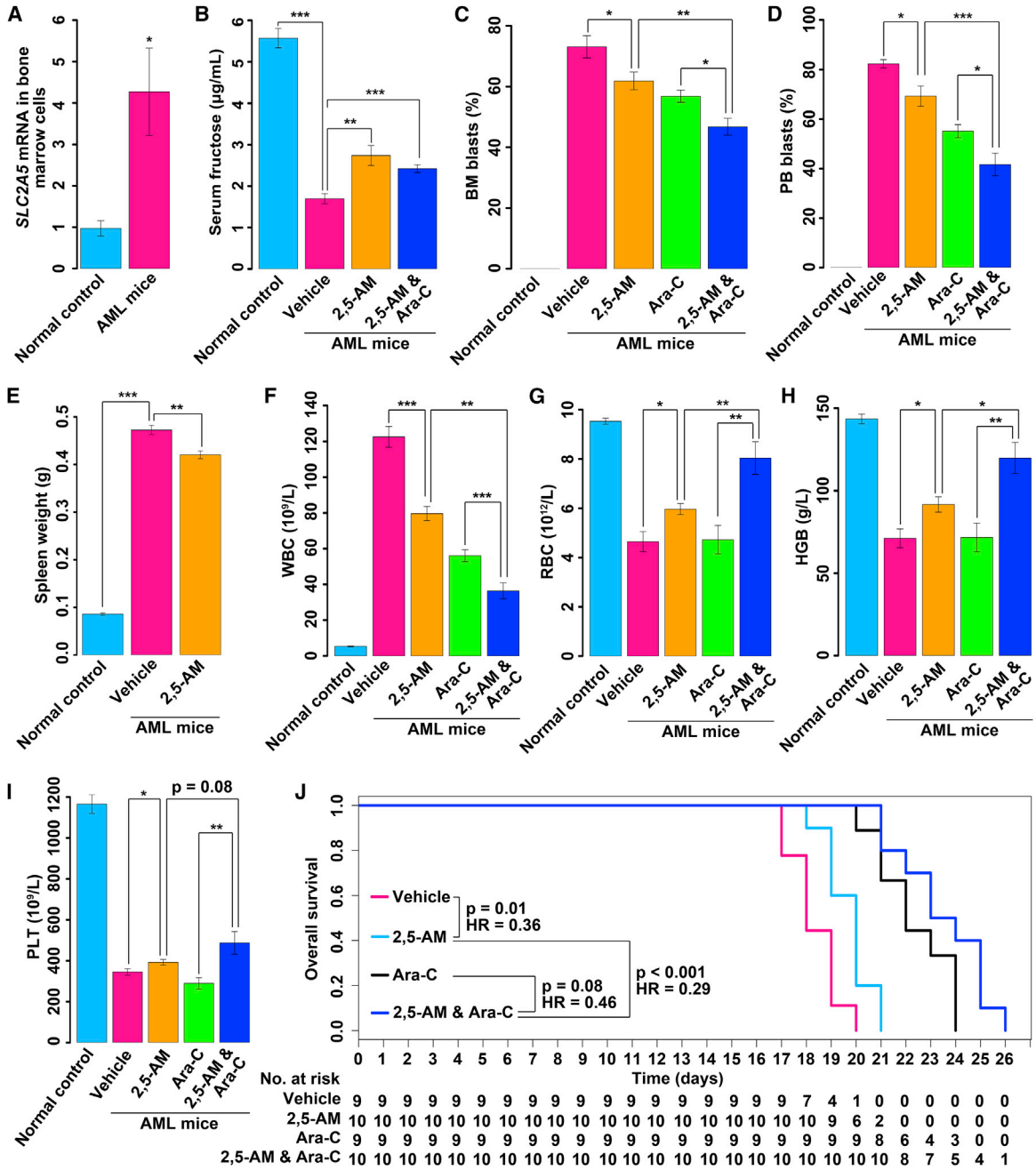

Figure 6. Enhanced Fructose Utilization and the Therapeutic Potential of Pharmacological Blockage of this Metabolic Pathway in AML Mice

(A) *SLC2A5* expression in bone marrow cells between normal controls (n = 6) and AML mice (n = 6).

(B) Serum fructose concentration measurements for normal controls (n = 6), AML mice treated with vehicle (n = 6), AML mice treated with 2,5-AM (n = 6), and AML mice treated with 2,5-AM + Ara-C (n = 6).

(C) The percentage of bone marrow (BM) blast cells in normal controls (n = 6), AML mice treated with vehicle (n = 6), AML mice treated with 2,5-AM (n = 6), AML mice treated with Ara-C (n = 6), and AML mice treated with 2,5-AM + Ara-C (n = 6).

(D) The percentage of peripheral blood (PB) blast cells in normal controls (n = 6), AML mice treated with vehicle (n = 6), AML mice treated with 2,5-AM (n = 6), AML mice treated with Ara-C (n = 6), and AML mice treated with 2,5-AM + Ara-C (n = 6).

(E) Spleen weight measurements for normal controls (n = 6), AML mice treated with vehicle (n = 6) and AML mice treated with 2,5-AM (n = 6).

(F) White blood cell (WBC) counts in PB for normal controls (n = 6), AML mice treated with vehicle (n = 8), AML mice treated with 2,5-AM (n = 8), AML mice treated with Ara-C (n = 6), and AML mice treated with 2,5-AM + Ara-C (n = 6).

(G) Red blood cell (RBC) counts in PB for normal controls (n = 6), AML mice treated with vehicle (n = 8), AML mice treated with 2,5-AM (n = 8), AML mice treated with Ara-C (n = 6), and AML mice treated with 2,5-AM + Ara-C (n = 6).

(legend continued on next page)

In the current study in vitro AML cell line models and an in vivo AML mouse model were chosen to investigate whether fructose, an alternative substrate for glycolysis, would exhibit enhanced utilization by AML cells and normal monocyte controls in a glucose-limiting environment. The AML cell lines were chosen to represent four different French-American-British subtypes, and to highlight a variety of mutations and individual different pathways leading toward leukemogenesis. We found that these four AML cell lines highly expressed GLUT5 and switched to fructose utilization under glucose-limiting conditions, whereas normal monocytes showed a low dependence on fructose for cell survival and growth. For AML mice, their bone marrow blast cells exhibited increased *SLC2A5* expression and elevated fructose utilization as measured by mRNA and serum levels, respectively.

Fructose has previously been reported to alter the glycan structures on the cell surface of tumor cells and increase their proliferative and invasive properties when compared with glucose in vitro (Monzavi-Karbassi et al., 2010). Our data demonstrated that altered fructose utilization plays a key role in AML progression as evidenced by an exacerbated leukemic phenotype regardless of the concentration of glucose present. In the fructose-containing media with or without glucose, AML cells with high *SLC2A5* expression showed elevated fructose uptake, increased proliferation and colony growth, and enhanced abilities of migration and invasion. As colony formation in soft agar is linked to cancer stem cell properties (Matsubara et al., 2013), the high *SLC2A5* expression may contribute to expansion of the leukemic stem cell compartment. Metabolic flux analysis demonstrated that high fructose utilization strongly activated glycolytic flux with increased pyruvate and lactate production in AML cells. The increased glycolytic activity has been implicated in promoting aggressiveness of cancer cells (Diers et al., 2012; Doherty and Cleveland, 2013). Consequently, enhanced fructose utilization or high *SLC2A5* expression in AML cells may be linked to poor outcomes in AML patients.

Evidence of this is provided in this study through analysis of five previously published gene expression datasets which showed that above-median/mean *SLC2A5* expression was associated with inferior overall survival. Analysis of serum fructose concentrations in 262 de novo AML patients revealed an association of serum fructose levels with the efficacy of inducing remission using standard AML 3 + 7 treatment. Those patients who had higher serum fructose concentrations had higher rates of CR compared with those with low or medium serum fructose levels. These results link enhanced AML cell fructose utilization to a worse patient clinical outcome. Of note, the investigation of the association between *SLC2A5* expression/fructose utilization and AML patient prognosis is a retrospective analysis. A blinded prospective study is needed to validate these findings.

In conclusion, the unique fructose utilization feature of AML cells provides a promising cancer target, and fructose inhibition may thus provide a viable, cell-cycle-independent therapy for AML. A fructose analog, 2,5-AM, was effective in alleviating the neoplastic phenotypes of AML cells in vitro and in vivo. We also observed a significant synergistic effect between 2,5-AM and Ara-C on the elimination of AML cells. It was noticeable that fructose utilization was heterogeneous in AML patients, as shown by the highly diverse expression of *SLC2A5* and serum fructose in these patients. Our findings suggested that only those AML patients whose blast cells highly expressed *SLC2A5* and exhibited enhanced fructose utilization would be able to obtain therapeutic benefit using a fructose utilization inhibitor in combination with a chemotherapeutic agent.

EXPERIMENTAL PROCEDURES

AML Cell Lines, Normal Monocytes, Reagents, and Antibodies

Four representative AML cell lines, U937, OCI-AML3, HL-60, and K562, were chosen for this study. U937 and OCI-AML3 were purchased from American Type Culture Collection, and HL-60 and K562 were obtained from the National Cancer Institute. All cell lines were maintained in RPMI 1640 (Life Technologies) supplemented with 10% fetal bovine serum (FBS, Life Technologies) and antibiotics. A total of four different control samples of normal monocytes were enrolled in this study. One control sample was purchased from STEMCELL Technologies. The remaining controls were provided by three healthy volunteers. All the normal monocytes were used to perform assays immediately after arrival. Reagents used in the study included D-fructose (Sigma-Aldrich), D-glucose (Sigma-Aldrich), GLUT5 antibody (Santa Cruz), actin antibody (LI-COR Biosciences), fructose analog 2,5-anhydro-D-mannitol (Santa Cruz), and antileukemic agent arabinofuranosyl cytidine (Sigma-Aldrich).

Knockdown of *SLC2A5* Expression by RNAi in AML Cells

The fructose transporter gene *SLC2A5* was knocked down in K562 AML cells using RNAi technology. K562 cells were transfected with a small interfering RNA (siRNA) targeting *SLC2A5* (QIAGEN) or a non-targeting control siRNA (QIAGEN). Transfections were conducted using a Lipofectamine 3000 Transfection Reagent Kit (Life Technologies) following the manufacturer's protocol. After 96 hr incubation, cells were harvested and protein extracts were prepared for western blot analysis of GLUT5 expression. Meanwhile, the proliferation of the transfected cells fed with fructose or glucose was measured at different time points using a Cell Counting Kit-8 (Dojindo Molecular Technologies) following the manufacturer's protocol.

Overexpression of *SLC2A5* in AML Cells

Enforced expression of *SLC2A5* in AML cells was achieved using a retrovirus system consisting of MigR1 vector (a gift from Warren Pear) (Pear et al., 1998), vesicular stomatitis virus G protein, and gag/pol packaging vectors. A more detailed description of the procedure is provided in the Supplemental Information procedures.

Measurement of Serum Fructose

Serum fructose concentrations of AML patients and healthy volunteers were examined as part of the metabolomic study involving a large series of AML cases described previously (Chen et al., 2014; Wang et al., 2013). A total of

(H) Hemoglobin (HGB) measurements in PB for normal controls (n = 6), AML mice treated with vehicle (n = 8), AML mice treated with 2,5-AM (n = 8), AML mice treated with Ara-C (n = 6), and AML mice treated with 2,5-AM + Ara-C (n = 6).

(I) Platelet (PLT) counts in PB for normal controls (n = 6), AML mice treated with vehicle (n = 8), AML mice treated with 2,5-AM (n = 8), AML mice treated with Ara-C (n = 6), and AML mice treated with 2,5-AM + Ara-C (n = 6).

(J) Overall survival curves of AML mice treated with vehicle (n = 9), AML mice treated with 2,5-AM (n = 10), AML mice treated with Ara-C (n = 9), and AML mice treated with 2,5-AM + Ara-C (n = 10). HR, hazard ratio.

Error bars represent mean ± SEM. *$p < 0.05$, **$p < 0.01$, ***$p < 0.001$ (Student's t test).

See also Figure S6 and Table S5.

400 de novo AML patients and 446 age- and gender-matched healthy controls were enrolled in this study from the hematology centers of Shanghai, Hangzhou, Suzhou, Shenyang, Nanjing, Dalian, and Beijing. The clinical data of these subjects were reported in our previously published study (Chen et al., 2014). For therapeutic response analysis, 262 cases who received standard DA regimen (daunorubicin 40 mg/m^2/day for 3 days and Ara-C 100 mg/m^2/day for 7 days) in remission-induction phase were analyzed. All participants provided informed written consent in accordance with the regulation of the institutional review boards of the related universities/hospitals in agreement with the Declaration of Helsinki. Mouse peripheral blood serum samples were collected as mentioned below.

Serum samples of human subjects and mice were analyzed using GC-TOFMS as described previously (Chen et al., 2014; Wang et al., 2013). Fructose was identified by library searching and then confirmed by the standard (Sigma-Aldrich). Calibration of fructose concentration data was performed as reported previously (Chen et al., 2014). The absolute concentration of serum fructose was determined from the calibration curve.

Analysis of ^{13}C-Labeled Fructose/Glucose Uptake and ^{13}C-Labeled Fructose-Derived Metabolites by GC-TOFMS

To assay the fructose/glucose uptake and fructose-derived metabolites, cells were cultured in glucose-free RPMI 1640 medium supplemented with 10% dialyzed FBS and 6 mM [U-$^{13}C_6$] fructose (Cambridge Isotope Laboratories) or 6 mM [U-$^{13}C_6$] glucose (Cambridge Isotope Laboratories). After incubation for 96 hr, cell culture media were collected. Then, 20 μL of cell medium was used for extraction of metabolites of ^{13}C-fructose and ^{13}C-glucose. Metabolite derivatization and GC-TOFMS assays were performed as described previously (Chen et al., 2014; Wang et al., 2013). ^{13}C-Fructose and ^{13}C-glucose were monitored using ions at m/z 220 and 323, respectively. ^{13}C-Fructose-derived metabolites, including ^{13}C-pyruvate, ^{13}C-lactate, and ^{13}C-alanine were monitored at m/z 177, 222, and 118, respectively. Metabolite consumption and release were calculated based on the algorithm reported previously (Jain et al., 2012).

AML Mouse Study

We enrolled five groups of mice in this study, including a normal control group, AML mice treated with vehicle (vehicle group), AML mice treated with the fructose utilization inhibitor 2,5-AM (2,5-AM group), AML mice treated with Ara-C (Ara-C group) and AML mice treated with 2,5-AM and Ara-C (2,5-AM + Ara-C group). Eight-week-old female BALB/c mice were selected for this study. Mice were maintained under specific pathogen-free conditions, kept on a 12-hr light-dark cycle, and fed a normal diet. AML mice were generated using a previously reported procedure (Wang et al., 2011) with minor modifications. In brief, 1 × 10^5 GFP-positive murine leukemic cells (splenic cells) with *AML1-ETO* and mutated *C-KIT* were injected into the tail vein of each sublethally irradiated (3.5 Gy) mouse. For the 2,5-AM treatment group, the reagent was dissolved in physiological saline and intraperitoneally injected into AML mice at a dose of 150 mg/kg/day at day 5 after leukemic cell transplantation until the mice were either killed or died. For the Ara-C treatment group, Ara-C was dissolved in physiological saline and intraperitoneally injected into AML mice at a dose of 25 mg/kg/day at day 3 after leukemic cell transplantation for 5 days. For the 2,5-AM + Ara-C treatment group, 2,5-AM and Ara-C were given to the mice according to the methods described in the 2,5-AM group and Ara-C group. The same volume of physiological saline was given to the vehicle group. Seventeen days after leukemic cell transplantation, five groups of mice, including six normal controls, eight AML mice treated with vehicle, eight AML mice treated with 2,5-AM, six AML mice treated with Ara-C, and six mice treated with 2,5-AM and Ara-C, were killed to obtain peripheral blood, serum, bone marrow, and spleen for analysis. In addition, nine AML mice treated with vehicle, ten AML mice treated with 2,5-AM, nine AML mice treated with Ara-C, and ten AML mice treated with a combination of 2,5-AM and Ara-C were maintained for investigating overall survival. The animal experiments were approved by the Department of Animal Experimentation at Shanghai Jiao Tong University School of Medicine.

Statistical Analysis

Significant differences between groups were determined using the Student's t test. The difference for survival time was assessed using log rank test. Meta-analysis of survival data was performed using the survcomp package in R software (version 2.15.0, www.r-project.org). The difference in therapeutic response among AML patient groups with distinct serum fructose levels was assessed using χ^2 test. The significance level was set at $p < 0.05$. The evaluation of synergistic effect between fructose analog 2,5-AM and Ara-C was executed in CompuSyn software (ComboSyn).

SUPPLEMENTAL INFORMATION

Supplemental Information includes Supplemental Experimental Procedures, six figures, and five tables and can be found with this article online at http://dx.doi.org/10.1016/j.ccell.2016.09.006.

AUTHOR CONTRIBUTIONS

W.J. and S.-J.C. were the principal investigators of this study, and conceived the research together with W.-L.C.; W.-L.C. performed the molecular and cellular biology experiments and analyzed the data; W.-L.C., A.Z., J.L., and Q.C. did serum fructose measurement; G.X., M.S., and L.Z. carried out ^{13}C-labeled sugar uptake and glycolytic flux assays; Z. Chen and S.-J.C. provided the clinical data that involved 400 AML patients for this study; W.-L.C., Y.-Y.W., and L.X. performed the mouse study; W.-L.C, R.W., and Y.N. performed the statistical analysis; W.-L.C. and W.J. wrote the manuscript; C.R. and Z. Cheng contributed to manuscript revision.

ACKNOWLEDGMENTS

This work was partially supported by NIH/NCI grant P30 CA071789 and the National Natural Science Foundation of China for Excellent Young Scholars Grant 81222004. We thank Dr. Peter J.M. Valk (Erasmus University Medical Center, Rotterdam, the Netherlands) and Dr. Jonathan R. Pollack (Stanford University, Stanford, USA) for sharing the clinical data of microarray datasets GEO: GSE1159 and GSE425, respectively.

Received: November 17, 2015
Revised: April 8, 2016
Accepted: September 13, 2016
Published: October 13, 2016

REFERENCES

Aries, I.M., Hansen, B.R., Koch, T., van den Dungen, R., Evans, W.E., Pieters, R., and den Boer, M.L. (2013). The synergism of MCL1 and glycolysis on pediatric acute lymphoblastic leukemia cell survival and prednisolone resistance. Haematologica *98*, 1905–1911.

Barone, S., Fussell, S.L., Singh, A.K., Lucas, F., Xu, J., Kim, C., Wu, X., Yu, Y., Amlal, H., Seidler, U., et al. (2009). Slc2a5 (Glut5) is essential for the absorption of fructose in the intestine and generation of fructose-induced hypertension. J. Biol. Chem. *284*, 5056–5066.

Bullinger, L., Dohner, K., Bair, E., Frohling, S., Schlenk, R.F., Tibshirani, R., Dohner, H., and Pollack, J.R. (2004). Use of gene-expression profiling to identify prognostic subclasses in adult acute myeloid leukemia. N. Engl. J. Med. *350*, 1605–1616.

Burant, C.F., Takeda, J., Brot-Laroche, E., Bell, G.I., and Davidson, N.O. (1992). Fructose transporter in human spermatozoa and small intestine is GLUT5. J. Biol. Chem. *267*, 14523–14526.

Cairns, R.A., Harris, I.S., and Mak, T.W. (2011). Regulation of cancer cell metabolism. Nat. Rev. Cancer *11*, 85–95.

Chen, W.L., Wang, J.H., Zhao, A.H., Xu, X., Wang, Y.H., Chen, T.L., Li, J.M., Mi, J.Q., Zhu, Y.M., Liu, Y.F., et al. (2014). A distinct glucose metabolism signature of acute myeloid leukemia with prognostic value. Blood *124*, 1645–1654.

Diers, A.R., Broniowska, K.A., Chang, C.F., and Hogg, N. (2012). Pyruvate fuels mitochondrial respiration and proliferation of breast cancer cells: effect of monocarboxylate transporter inhibition. Biochem. J. *444*, 561–571.

Doherty, J.R., and Cleveland, J.L. (2013). Targeting lactate metabolism for cancer therapeutics. J. Clin. Invest. *123*, 3685–3692.

Ferrara, F., and Schiffer, C.A. (2013). Acute myeloid leukaemia in adults. Lancet *381*, 484–495.

Herst, P.M., Howman, R.A., Neeson, P.J., Berridge, M.V., and Ritchie, D.S. (2011). The level of glycolytic metabolism in acute myeloid leukemia blasts at diagnosis is prognostic for clinical outcome. J. Leukoc. Biol. *89*, 51–55.

Hulleman, E., Kazemier, K.M., Holleman, A., VanderWeele, D.J., Rudin, C.M., Broekhuis, M.J., Evans, W.E., Pieters, R., and Den Boer, M.L. (2009). Inhibition of glycolysis modulates prednisolone resistance in acute lymphoblastic leukemia cells. Blood *113*, 2014–2021.

Jain, M., Nilsson, R., Sharma, S., Madhusudhan, N., Kitami, T., Souza, A.L., Kafri, R., Kirschner, M.W., Clish, C.B., and Mootha, V.K. (2012). Metabolite profiling identifies a key role for glycine in rapid cancer cell proliferation. Science *336*, 1040–1044.

Jang, M., Kim, S.S., and Lee, J. (2013). Cancer cell metabolism: implications for therapeutic targets. Exp. Mol. Med. *45*, e45.

Liu, H., Huang, D., McArthur, D.L., Boros, L.G., Nissen, N., and Heaney, A.P. (2010). Fructose induces transketolase flux to promote pancreatic cancer growth. Cancer Res. *70*, 6368–6376.

Losman, J.A., Looper, R.E., Koivunen, P., Lee, S., Schneider, R.K., McMahon, C., Cowley, G.S., Root, D.E., Ebert, B.L., and Kaelin, W.G., Jr. (2013). (R)-2-hydroxyglutarate is sufficient to promote leukemogenesis and its effects are reversible. Science *339*, 1621–1625.

Lum, J.J., Bui, T., Gruber, M., Gordan, J.D., DeBerardinis, R.J., Covello, K.L., Simon, M.C., and Thompson, C.B. (2007). The transcription factor HIF-1alpha plays a critical role in the growth factor-dependent regulation of both aerobic and anaerobic glycolysis. Genes Dev. *21*, 1037–1049.

Martincic, D., and Hande, K.R. (2005). Topoisomerase II inhibitors. Cancer Chemother. Biol. Response Modif. *22*, 101–121.

Matsubara, S., Ding, Q., Miyazaki, Y., Kuwahata, T., Tsukasa, K., and Takao, S. (2013). mTOR plays critical roles in pancreatic cancer stem cells through specific and stemness-related functions. Sci. Rep. *3*, 3230.

Metzeler, K.H., Hummel, M., Bloomfield, C.D., Spiekermann, K., Braess, J., Sauerland, M.C., Heinecke, A., Radmacher, M., Marcucci, G., Whitman, S.P., et al. (2008). An 86-probe-set gene-expression signature predicts survival in cytogenetically normal acute myeloid leukemia. Blood *112*, 4193–4201.

Momparler, R.L. (2013). Optimization of cytarabine (ARA-C) therapy for acute myeloid leukemia. Exp. Hematol. Oncol. *2*, 20.

Monzavi-Karbassi, B., Hine, R.J., Stanley, J.S., Ramani, V.P., Carcel-Trullols, J., Whitehead, T.L., Kelly, T., Siegel, E.R., Artaud, C., Shaaf, S., et al. (2010). Fructose as a carbon source induces an aggressive phenotype in MDA-MB-468 breast tumor cells. Int. J. Oncol. *37*, 615–622.

Patel, J.P., Gonen, M., Figueroa, M.E., Fernandez, H., Sun, Z., Racevskis, J., Van Vlierberghe, P., Dolgalev, I., Thomas, S., Aminova, O., et al. (2012). Prognostic relevance of integrated genetic profiling in acute myeloid leukemia. N. Engl. J. Med. *366*, 1079–1089.

Pear, W.S., Miller, J.P., Xu, L., Pui, J.C., Soffer, B., Quackenbush, R.C., Pendergast, A.M., Bronson, R., Aster, J.C., Scott, M.L., and Baltimore, D. (1998). Efficient and rapid induction of a chronic myelogenous leukemia-like myeloproliferative disease in mice receiving P210 bcr/abl-transduced bone marrow. Blood *92*, 3780–3792.

Raez, L.E., Papadopoulos, K., Ricart, A.D., Chiorean, E.G., Dipaola, R.S., Stein, M.N., Rocha Lima, C.M., Schlesselman, J.J., Tolba, K., et al. (2013). A phase I dose-escalation trial of 2-deoxy-D-glucose alone or combined with docetaxel in patients with advanced solid tumors. Cancer Chemother. Pharmacol. *71*, 523–530.

Stirewalt, D.L., Meshinchi, S., Kopecky, K.J., Fan, W., Pogosova-Agadjanyan, E.L., Engel, J.H., Cronk, M.R., Dorcy, K.S., McQuary, A.R., Hockenbery, D., et al. (2008). Identification of genes with abnormal expression changes in acute myeloid leukemia. Genes Chromosomes Cancer *47*, 8–20.

Stirewalt, D.L., Pogosova-Agadjanyan, E.L., and Ochsenreither, S.K. (2012). http://www.ncbi.nlm.nih.gov/geo/query/acc.cgi?acc=GSE37307.

Tabe, Y., and Konopleva, M. (2014). Advances in understanding the leukaemia microenvironment. Br. J. Haematol. *164*, 767–778.

Tiziani, S., Kang, Y., Harjanto, R., Axelrod, J., Piermarocchi, C., Roberts, W., and Paternostro, G. (2013). Metabolomics of the tumor microenvironment in pediatric acute lymphoblastic leukemia. PLoS One *8*, e82859.

Valk, P.J., Verhaak, R.G., Beijen, M.A., Erpelinck, C.A., Barjesteh van Waalwijk van Doorn-Khosrovani, S., Boer, J.M., Beverloo, H.B., Moorhouse, M.J., van der Spek, P.J., Lowenberg, B., and Delwel, R. (2004). Prognostically useful gene-expression profiles in acute myeloid leukemia. N. Engl. J. Med. *350*, 1617–1628.

Vijayaraghavan, R., Kumar, D., Dube, S.N., Singh, R., Pandey, K.S., Bag, B.C., Kaushik, M.P., Sekhar, K., Dwarakanath, B.S., and Ravindranath, T. (2006). Acute toxicity and cardio-respiratory effects of 2-deoxy-D-glucose: a promising radio sensitiser. Biomed. Environ. Sci. *19*, 96–103.

Wang, Y.Y., Zhao, L.J., Wu, C.F., Liu, P., Shi, L., Liang, Y., Xiong, S.M., Mi, J.Q., Chen, Z., Ren, R., and Chen, S.J. (2011). C-KIT mutation cooperates with full-length AML1-ETO to induce acute myeloid leukemia in mice. Proc. Natl. Acad. Sci. USA *108*, 2450–2455.

Wang, J.H., Chen, W.L., Li, J.M., Wu, S.F., Chen, T.L., Zhu, Y.M., Zhang, W.N., Li, Y., Qiu, Y.P., Zhao, A.H., et al. (2013). Prognostic significance of 2-hydroxyglutarate levels in acute myeloid leukemia in China. Proc. Natl. Acad. Sci. USA *110*, 17017–17022.

Yang, J., Dowden, J., Tatibouet, A., Hatanaka, Y., and Holman, G.D. (2002). Development of high-affinity ligands and photoaffinity labels for the D-fructose transporter GLUT5. Biochem. J. *367*, 533–539.

Zebisch, A., Wolfler, A., Fried, I., Wolf, O., Lind, K., Bodner, C., Haller, M., Drasche, A., Pirkebner, D., Matallanas, D., et al. (2012). Frequent loss of RAF kinase inhibitor protein expression in acute myeloid leukemia. Leukemia *26*, 1842–1849.

Zhao, F.Q., and Keating, A.F. (2007). Functional properties and genomics of glucose transporters. Curr. Genomics *8*, 113–128.

Zhao, Y., Butler, E.B., and Tan, M. (2013). Targeting cellular metabolism to improve cancer therapeutics. Cell Death Dis. *4*, e532.

Cancer Cell, Volume *30*

Supplemental Information

Enhanced Fructose Utilization Mediated by *SLC2A5* Is a Unique Metabolic Feature of Acute Myeloid Leukemia with Therapeutic Potential

Wen-Lian Chen, Yue-Ying Wang, Aihua Zhao, Li Xia, Guoxiang Xie, Mingming Su, Linjing Zhao, Jiajian Liu, Chun Qu, Runmin Wei, Cynthia Rajani, Yan Ni, Zhen Cheng, Zhu Chen, Sai-Juan Chen, and Wei Jia

Supplemental Information

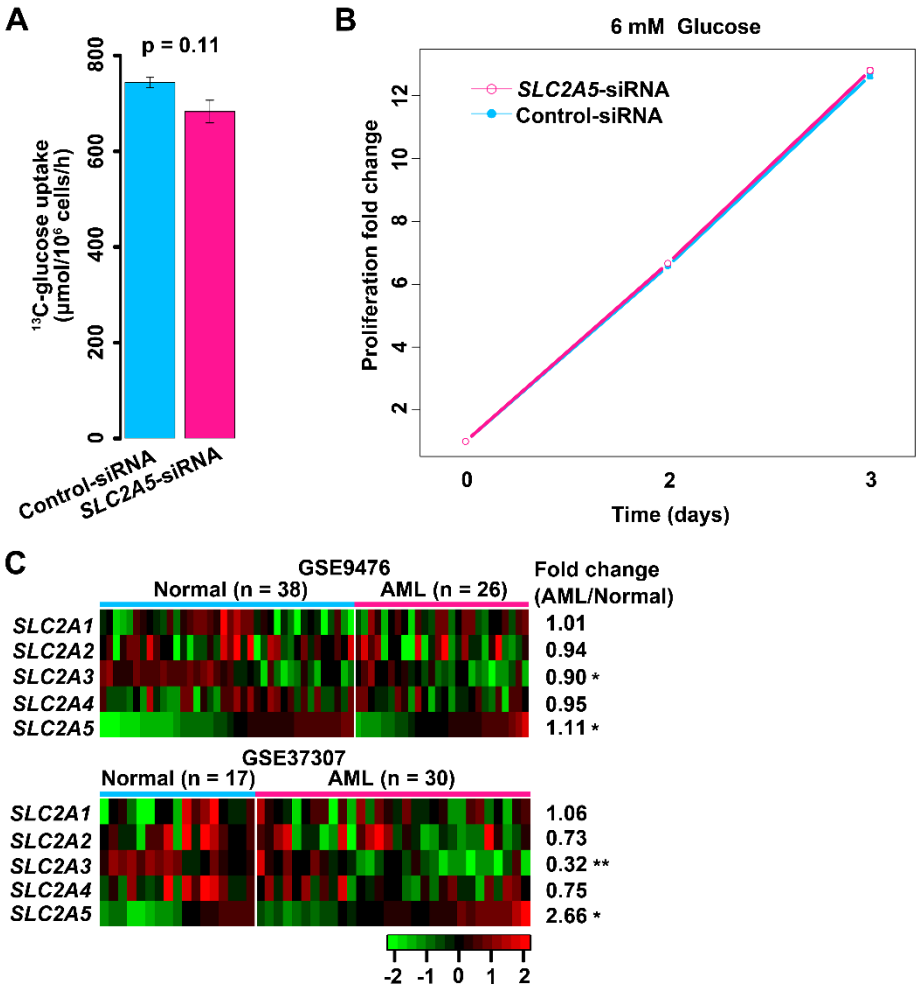

Figure S1. Related to Figure 1. (A,B) The influence of *SLC2A5* deletion on glucose uptake and glucose-induced proliferation in K562 cells; (C) The sugar transporter gene expression between normal hematopoietic cells and primary AML blast cells.

(A) Uptake of ^{13}C-glucose by K562 cells with or without *SLC2A5* deletion.

(B) Proliferation of K562 cells with or without *SLC2A5* deletion in complete medium containing 6 mM glucose.

(C) The expression of sugar transporter genes including *SLC2A1*, *SLC2A2*, *SLC2A3*, *SLC2A4* and *SLC2A5* between normal hematopoietic cells of healthy controls and AML blast cells of patients. The data were taken from public microarray database.

Error bars represent mean ± SEM. * $p < 0.05$, ** $p < 0.01$ (Student's t test).

Table S1. Related to Figure 1. Characteristics of AML cell lines included in the study.

Cell line	FAB	Cytogenetics	Genetic aberrance	Incidence	Prognosis
U937	M5	t(10;11)(p13;q14)	*CALM*/*AF10*	5% (Lillington et al., 1998)	High relapse risk
OCI-AML3	M4	Normal karyotype	Mutated *NPM1* and *DNMT3A*	30% (Lowenberg, 2008)	Poor survival; High relapse risk
HL-60	M2	Hypotetraploid	Amplified *c-Myc*	4% (Bruckert et al., 2000)	Intermediate risk
K562	M6	t(9;22)(q34;q11)	*BCR*/*ABL*	1-3% (Keung et al., 2004)	Poor risk; High relapse risk

Table S2. Related to Figure 1. Spearman correlation analysis between *SLC2A5* expression and fusion genes/gene mutations.

Fusion gene/gene mutation	GSE1159 (n = 260)		GSE425 (n = 111)		TCGA data (n = 173)	
	Correlation r	p	Correlation r	p	Correlation r	p
PML-RARA	-0.32	< 0.001	-0.33	< 0.001	/	/
AML1-ETO	0.26	< 0.001	0.28	0.003	/	/
CBFβ-MYH11	-0.18	0.004	-0.13	0.16	/	/
FLT3-ITD	0.20	0.001	0.03	0.80	/	/
CEBPA[ζ]	-0.26	< 0.001	/	/	/	/
NPM1	0.20	0.001	/	/	/	/
RUNX1	/	/	/	/	0.21	0.01

[ζ]Biallelic CEBPA mutations.

"/" indicates not available.

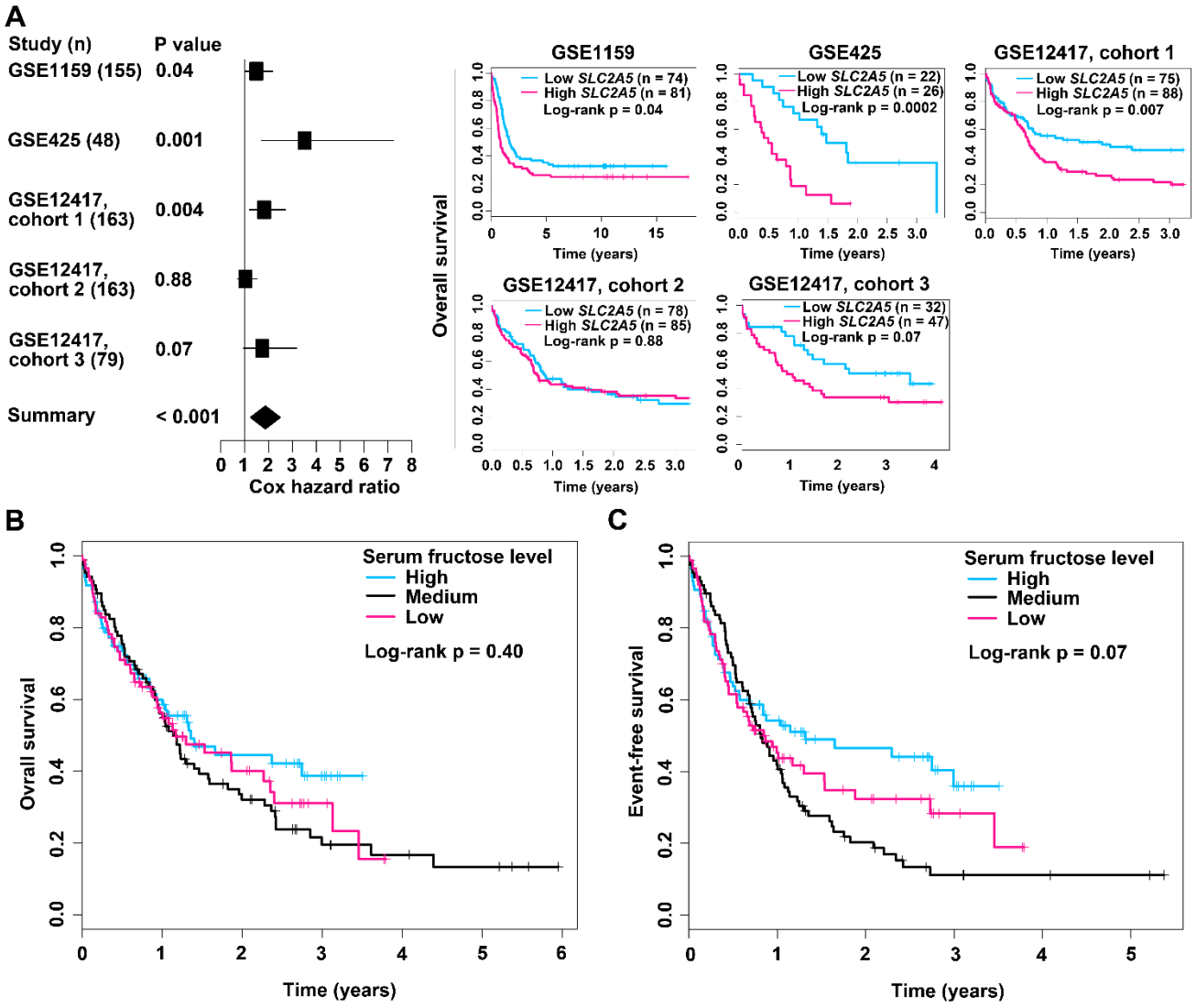

Figure S2. Related to Figure 2. The prognostic value analysis of different *SLC2A5* expression levels and distinct serum fructose concentrations in AML patients.

(A) (Left) Meta-analysis of Cox hazard ratio of *SLC2A5* expression levels in 5 data sets. The categorical values of *SLC2A5*, divided by the mean *SLC2A5* in each data set, were used in the analysis. (Right) Kaplan-Meier survival curves of AML patients of 5 data sets. Patients of each data set were divided into 2 groups using the mean *SLC2A5* expression as the cut-off value.

(B) Overall survival of 3 groups of AML patients divided by distinct serum fructose concentrations.

(C) Event-free survival of 3 groups of AML patients divided by distinct serum fructose concentrations.

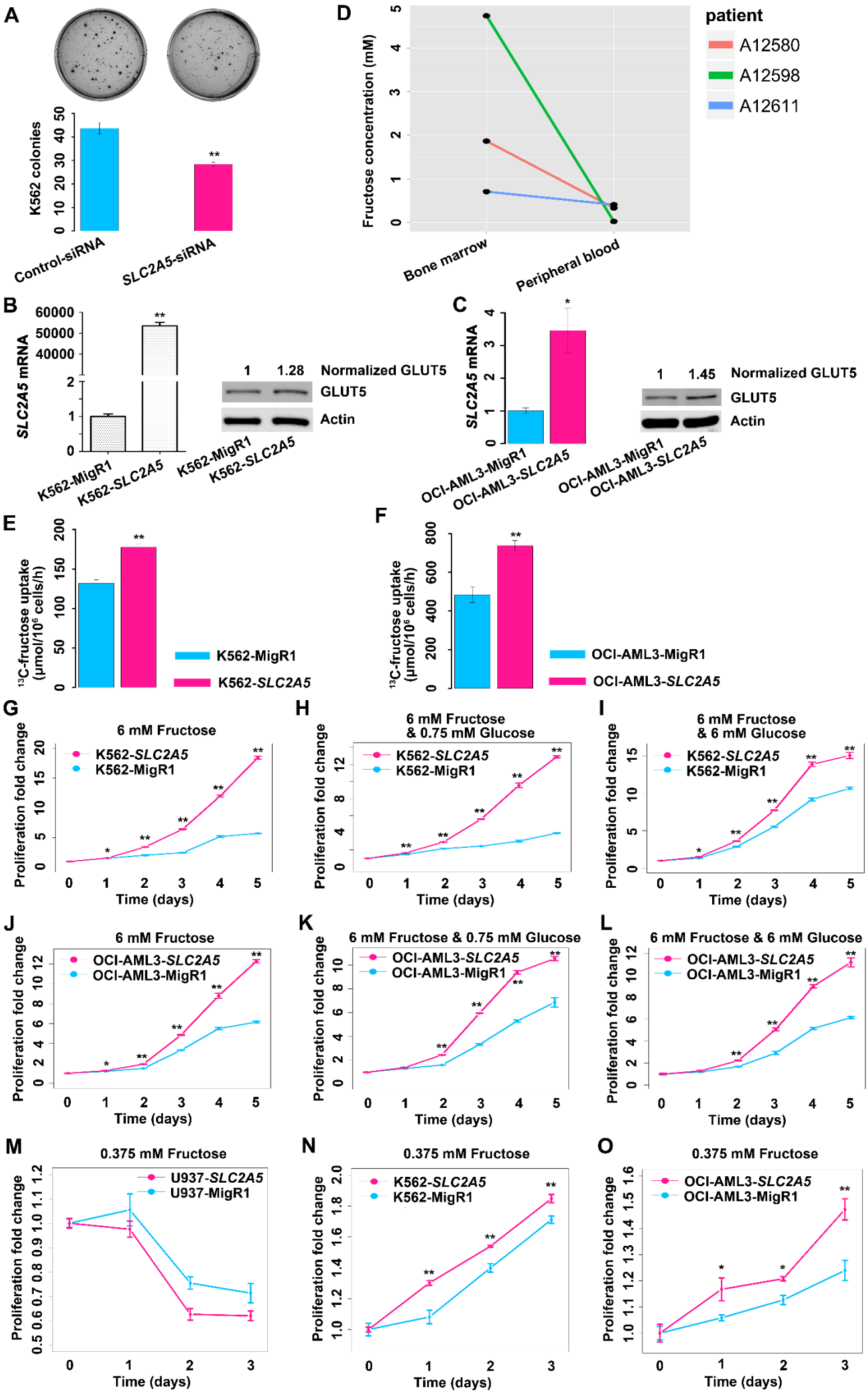
A
K562 colonies
Control-siRNA
SLC2A5-siRNA
D
Fructose concentration (mM)
Bone marrow
Peripheral blood
patient
A12580
A12598
A12611
B
SLC2A5 mRNA
K562-MigR1
K562-SLC2A5
1
1.28
Normalized GLUT5
GLUT5
Actin
C
SLC2A5 mRNA
OCI-AML3-MigR1
OCI-AML3-SLC2A5
1
1.45
Normalized GLUT5
GLUT5
Actin
E
13C-fructose uptake (µmol/10^6 cells/h)
K562-MigR1
K562-SLC2A5
F
13C-fructose uptake (µmol/10^6 cells/h)
OCI-AML3-MigR1
OCI-AML3-SLC2A5
G
6 mM Fructose
K562-SLC2A5
K562-MigR1
Proliferation fold change
Time (days)
H
6 mM Fructose & 0.75 mM Glucose
I
6 mM Fructose & 6 mM Glucose
J
6 mM Fructose
OCI-AML3-SLC2A5
OCI-AML3-MigR1
K
6 mM Fructose & 0.75 mM Glucose
L
6 mM Fructose & 6 mM Glucose
M
0.375 mM Fructose
U937-SLC2A5
U937-MigR1
N
0.375 mM Fructose
O
0.375 mM Fructose

Figure S3. Related to Figure 3. Enhanced fructose utilization mediated by *SLC2A5* promotes AML cell growth.

(A) Colony formation of K562 cells without or with suppressed *SLC2A5* expression. Cells were seeded at a density of 3000/well and fed with complete medium containing 6 mM fructose. Colonies were analyzed at day 30.

(B) Analysis of the expression of *SLC2A5*/GLUT5 in K562 cells transfected with the control MigR1 retrovirus (K562-MigR1) or MigR1-*SLC2A5* retrovirus (K562-*SLC2A5*) by Q-PCR and western blot respectively.

(C) Analysis of the expression of *SLC2A5*/GLUT5 in OCI-AML3 cells transfected with the control MigR1 retrovirus (OCI-AML3-MigR1) or MigR1-*SLC2A5* retrovirus (OCI-AML3-*SLC2A5*) by Q-PCR and western blot respectively.

(D) Fructose concentrations in paired peripheral blood and bone marrow samples from 3 AML patients.

(E) Uptake of ^{13}C-labeled fructose by K562-MigR1 and K562-*SLC2A5* cells.

(F) Uptake of ^{13}C-labeled fructose by OCI-AML3-MigR1 and OCI-AML3-*SLC2A5* cells.

(G-I) Proliferation of K562-MigR1 and K562-*SLC2A5* cells in complete media containing 6 mM fructose without glucose or with distinct levels of glucose.

(J-L) Proliferation of OCI-AML3-MigR1 and OCI-AML3-*SLC2A5* cells in complete media containing 6 mM fructose without glucose or with distinct levels of glucose.

(M) Proliferation of U937-MigR1 and U937-*SLC2A5* cells under 0.375 mM fructose condition.

(N) Proliferation of K562-MigR1 and K562-*SLC2A5* cells under 0.375 mM fructose condition.

(O) Proliferation of OCI-AML3-MigR1 and OCI-AML3-*SLC2A5* cells under 0.375 mM fructose condition.

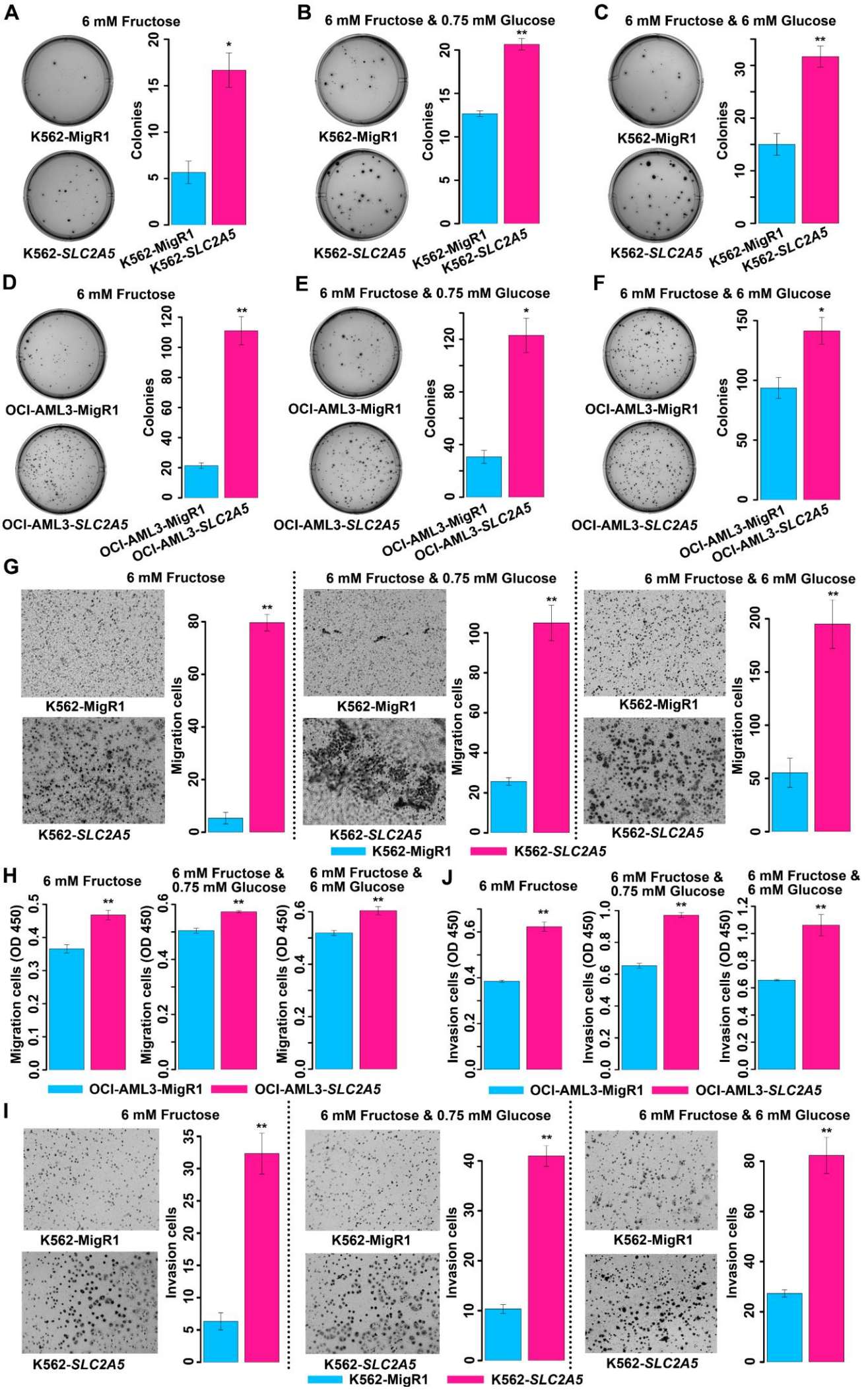
A
6 mM Fructose
K562-MigR1
K562-SLC2A5
Colonies
K562-MigR1
K562-SLC2A5
B
6 mM Fructose & 0.75 mM Glucose
K562-MigR1
K562-SLC2A5
Colonies
K562-MigR1
K562-SLC2A5
C
6 mM Fructose & 6 mM Glucose
K562-MigR1
K562-SLC2A5
Colonies
K562-MigR1
K562-SLC2A5
D
6 mM Fructose
OCI-AML3-MigR1
OCI-AML3-SLC2A5
Colonies
OCI-AML3-MigR1
OCI-AML3-SLC2A5
E
6 mM Fructose & 0.75 mM Glucose
OCI-AML3-MigR1
OCI-AML3-SLC2A5
Colonies
OCI-AML3-MigR1
OCI-AML3-SLC2A5
F
6 mM Fructose & 6 mM Glucose
OCI-AML3-MigR1
OCI-AML3-SLC2A5
Colonies
OCI-AML3-MigR1
OCI-AML3-SLC2A5
G
6 mM Fructose
K562-MigR1
K562-SLC2A5
Migration cells
6 mM Fructose & 0.75 mM Glucose
K562-MigR1
K562-SLC2A5
Migration cells
6 mM Fructose & 6 mM Glucose
K562-MigR1
K562-SLC2A5
Migration cells
K562-MigR1
K562-SLC2A5
H
6 mM Fructose
6 mM Fructose & 0.75 mM Glucose
6 mM Fructose & 6 mM Glucose
Migration cells (OD 450)
OCI-AML3-MigR1
OCI-AML3-SLC2A5
J
6 mM Fructose
6 mM Fructose & 0.75 mM Glucose
6 mM Fructose & 6 mM Glucose
Invasion cells (OD 450)
OCI-AML3-MigR1
OCI-AML3-SLC2A5
I
6 mM Fructose
K562-MigR1
K562-SLC2A5
Invasion cells
6 mM Fructose & 0.75 mM Glucose
K562-MigR1
K562-SLC2A5
Invasion cells
6 mM Fructose & 6 mM Glucose
K562-MigR1
K562-SLC2A5
Invasion cells
K562-MigR1
K562-SLC2A5

Figure S4. Related to Figure 3. Enhanced fructose utilization mediated by *SLC2A5* increases colony growth and migratory/invasive tendency of AML cells.

(A-C) Colony formation of K562-MigR1 and K562-*SLC2A5* cells in soft agar fed with complete media containing 6 mM fructose without glucose or with distinct levels of glucose. Cells were seeded at a density of 1,600/well (A) or 1,200/well (B) or 800/well (C). Colonies were assayed at day 23 (P and Q) or day 16 (R).

(D-F) Colony formation of OCIAML3-MigR1 and OCIAML3-*SLC2A5* cells in soft agar fed with complete media containing 6 mM fructose without glucose or with distinct levels of glucose. Cells were seeded at a density of 4,000/well (D) or 3,000/well (E) or 2,000/well (F). Colonies were assayed at day 16.

(G) Migration of K562-MigR1 and K562-*SLC2A5* cells fed with complete medium containing 6 mM fructose without glucose or with distinct levels of glucose.

(H) Migration of OCI-AML3-MigR1 and OCI-AML3-*SLC2A5* cells fed with complete medium containing 6 mM fructose without glucose or with distinct levels of glucose.

(I) Invasion of K562-MigR1 and K562-*SLC2A5* cells fed with complete medium containing 6 mM fructose without glucose or with distinct levels of glucose.

(J) Invasion of OCI-AML3-MigR1 and OCI-AML3-*SLC2A5* cells fed with complete medium containing 6 mM fructose without glucose or with distinct levels of glucose.

Error bars represent mean ± SEM. * $p < 0.05$, ** $p < 0.01$ (Student's t test).

Table S3. Related to Figure 3. Fructose concentrations in unpaired peripheral blood and bone marrow samples from patients with hematological malignancies.

Patient ID	Disease	Sample	Fructose (mM)	Fructose, median (range) (mM)	Wilcoxon p value
619	NHL	Peripheral blood	0.925	0.176 (0-1.456)	0.007
620	NHL	Peripheral blood	0.527		
621	NHL	Peripheral blood	0		
622	NHL	Peripheral blood	0.030		
623	AML	Peripheral blood	0.210		
624	NHL	Peripheral blood	0.138		
625	AML	Peripheral blood	0		
626	MM	Peripheral blood	0.143		
627	AML	Peripheral blood	1.043		
629	ALL	Peripheral blood	1.456		
630	AML	Bone marrow	5.162	1.492 (0.337-5.168)	
631	NHL	Bone marrow	1.192		
632	AML	Bone marrow	1.492		
633	AML	Bone marrow	5.168		
634	NHL	Bone marrow	0.618		
635	NHL	Bone marrow	0.337		
636	AML	Bone marrow	2.707		

Abbreviation: NHL, Non-Hodgkin's lymphomas; MM, Multiple myeloma; ALL, Acute lymphoblastic leukemia.

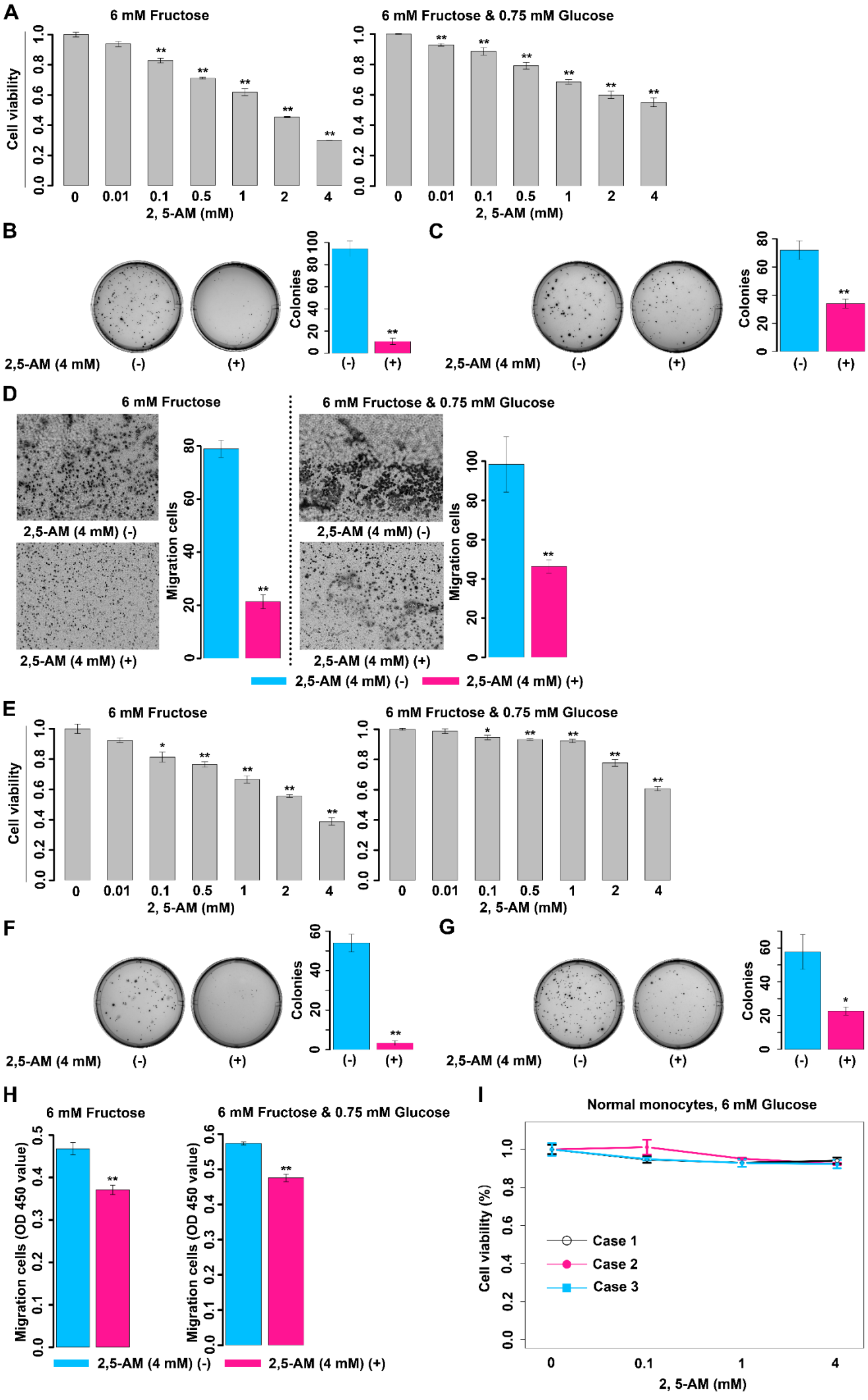
A
6 mM Fructose
6 mM Fructose & 0.75 mM Glucose
Cell viability
2, 5-AM (mM)
B
C
Colonies
2,5-AM (4 mM)
(-)
(+)
D
6 mM Fructose
6 mM Fructose & 0.75 mM Glucose
2,5-AM (4 mM) (-)
2,5-AM (4 mM) (+)
Migration cells
E
F
G
H
Migration cells (OD 450 value)
I
Normal monocytes, 6 mM Glucose
Cell viability (%)
Case 1
Case 2
Case 3

Figure S5. Related to Figure 5. Response of K562-*SLC2A5*, OCI-AML3-*SLC2A5* and normal monocytes to pharmacological blockage of fructose utilization.

(A) Suppressed proliferation of K562-*SLC2A5* cells treated with the fructose analogue 2,5-AM. Two carbon source conditions, 6 mM fructose and 6 mM fructose plus 0.75 mM glucose, were tested. P values were obtained by comparison with the proliferation of K562-*SLC2A5* cells in 0 mM 2,5-AM.

(B-C) The colony growth of K562-*SLC2A5* cells in soft agar under the condition of 6 mM fructose (B) or 6 mM fructose plus 0.75 mM glucose (C) with or without 2,5-AM treatment. Cells were seeded at a density of 2,000/well (B) or 1,500/well (C). Colonies were assayed at day 26.

(D) Migration assay of K562-*SLC2A5* cells with or without 2,5-AM treatment in medium containing 6 mM fructose or 6 mM fructose plus 0.75 mM glucose.

(E) Suppressed proliferation of OCI-AML3-*SLC2A5* cells treated with the fructose analogue 2,5-AM. Two carbon source conditions, 6 mM fructose and 6 mM fructose plus 0.75 mM glucose, were tested. P values were obtained by comparison with the proliferation of OCI-AML3-*SLC2A5* cells in 0 mM 2,5-AM.

(F-G) The colony growth of OCI-AML3-*SLC2A5* cells in soft agar under the condition of 6 mM fructose (F) or 6 mM fructose plus 0.75 mM glucose (G) with or without 2,5-AM treatment. Cells were seeded at a density of 4,000/well (F) or 3,000/well (G). Colonies were assayed at day 18 (F) or day 20 (G).

(H) Migration assay of OCI-AML3-*SLC2A5* cells with or without 2,5-AM treatment in medium containing 6 mM fructose or 6 mM fructose plus 0.75 mM glucose.

(I) Influence of the fructose analogue 2,5-AM on the glucose-induced proliferation of normal monocytes.

Error bars represent mean ± SEM. * $p < 0.05$, ** $p < 0.01$(Student's t test).

Table S4. Related to Figure 5. Combination indices for combination of fructose analogue 2,5-AM and Ara-C in AML cell lines as computed by CompuSyn.

Cell line	Carbon source	Agent combination	Combination index			
			ED50	ED75	ED90	ED95
U937	6 mM Fructose	2,5-AM + Ara-C	0.84	0.74	0.64	0.59
OCI-AML3	6 mM Fructose	2,5-AM + Ara-C	0.66	0.61	0.59	0.58
HL-60	6 mM Fructose	2,5-AM + Ara-C	0.48	0.29	0.17	0.12
K562	6 mM Fructose	2,5-AM + Ara-C	0.36	0.30	0.25	0.22
U937	6 mM Fructose + 0.75 mM Glucose	2,5-AM + Ara-C	0.96	0.71	0.65	0.65
OCI-AML3	6 mM Fructose + 0.75 mM Glucose	2,5-AM + Ara-C	0.92	0.84	0.75	0.72
HL-60	6 mM Fructose + 0.75 mM Glucose	2,5-AM + Ara-C	0.69	0.39	0.22	0.15
K562	6 mM Fructose + 0.75 mM Glucose	2,5-AM + Ara-C	0.18	0.25	0.35	0.44

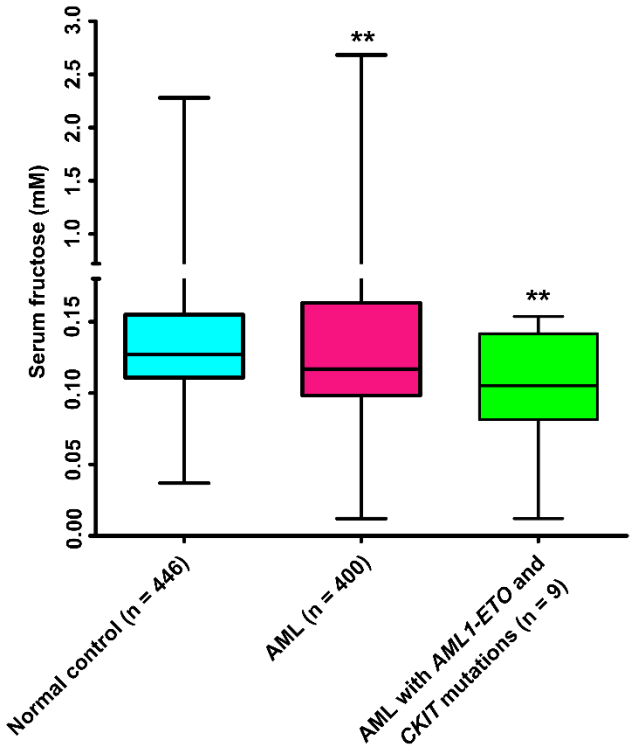

Figure S6. Related to Figure 6. Serum fructose concentrations in normal controls, patients with AML, and patients with AML harboring *AML1-ETO* and *C-KIT* mutations.

**p < 0.01 versus normal controls (Wilcoxon rank-sum test).

Table S5. Related to Figure 6. Description of the parameters among 5 mouse groups 17 days after leukemic cell transplantation.

Mouse group	PB blasts (%)	BM blasts (%)	Blasts in spleen (%)	WBC ($\times 10^9$/L)	RBC ($\times 10^{12}$/L)	HGB (g/L)	PLT ($\times 10^9$/L)	Spleen weight (g)
Normal controls (n = 6)	0	0	0	5.35 ± 0.09	9.53 ± 0.05	143.50 ± 1.10	1165.83 ± 17.06	0.09 ± 0.0008
Vehicle (n = 8)	82.33 ± 0.63	73.10 ± 1.36	89.57 ± 0.46	122.55 ± 1.93	4.65 ± 0.13	71.14 ± 1.88	345.33 ± 5.13	0.47 ± 0.004
2,5-AM (n = 8)	69.28 ± 1.53	61.85 ± 1.10	88.48 ± 0.30	79.63 ± 1.31	5.96 ± 0.07	91.63 ± 1.53	392.50 ± 4.62	0.42 ± 0.003
Ara-C (n = 6)	55.10 ± 0.99	56.82 ± 0.75	NA	56.03 ± 1.24	4.72 ± 0.22	71.67 ± 3.23	289.83 ± 10.25	NA
2,5-AM & Ara-C (n = 6)	41.66 ± 1.69	46.78 ± 1.04	89.48 ± 0.56	36.40 ± 1.66	8.04 ± 0.25	119.83 ± 3.53	487.25 ± 20.67	0.38 ± 0.005

All the parameter values were shown as mean ± standard error of mean.

PB, peripheral blood; BM, bone marrow; WBC, white blood cell; RBC, red blood cell; HGB, hemoglobin; PLT, platelet.

Supplemental experimental procedures

Cell Proliferation and Viability Assays

AML cells were harvested, rinsed twice in PBS and seeded into a 96-well plate at a density of 10,000 cells/well. For normal monocytes, cells were washed twice in PBS after thawing in a 37℃ water bath and then seeded into a 96-well plate at a density of 50,000 cells/well. Cells were grown in glucose-free RPMI 1640 (life technologies) containing 10% dialyzed FBS (dFBS, life technologies) (for AML cells) or 10% dFBS plus 5% human serum (Sigma) (for normal monocytes). For determination of the effect of fructose on cell proliferation, fructose solution was added in cells at a concentration range from 0 mM to 6 mM under defined glucose levels. For determination of the inhibitive effect of 2,5-anhydro-D-mannitol (2,5-AM) on fructose-induced cell proliferation, AML cells fed with 6 mM fructose, 6 mM fructose plus 0.75 mM glucose or 6 mM glucose were treated in a proper concentration range for this reagent. 2,5-AM and Ara-C were also used together to investigate their synergistic effects on AML cells. The drug concentration range for these experiments was set according to the suggested algorithm of CompuSyn software (ComboSyn, Inc., Paramus, NJ). Cell proliferation and cell viability were measured using a Cell Counting Kit-8 (CCK-8, Dojindo Laboratories) following the manufacturer's protocol at the time point(s) indicated in the figures or figure legends.

Overexpression of *SLC2A5* in AML Cells

A restriction endonuclease site of NcoI was added to the 2 ends of *SLC2A5* complementary DNA (cDNA) by polymerase chain reaction (PCR) with the following primers: 5'-CATGCCATGGAGCAACAGGATCAGAGC-3' and 5'-CATGCCATGGACTGTTCCGAAGTGACAGG-3'. The cDNA was then subcloned into MigR1 with the unique internal NcoI site. The insertion of the cDNA sequence into the vector was verified by Sanger sequencing. The retrovirus was produced as follows: empty MigR1 vector or MigR1 vector containing *SLC2A5* was cotransfected with VSVG and gag/pol plasmids into HEK293T cell using Lipofectamine 3000 (Life Technologies) following the manufacturer's instruction. Virus-containing supernatants were collected and filtered (0.45 μm filter) to remove cells. Subsequently, AML cells were infected with the control MigR1 virus or MigR1 virus expressing *SLC2A5* in the presence of 8 μg/mL polybrene. The green fluorescent protein (GFP)-positive cells were sorted 48 hours after infection using flow cytometry.

GLUT5 Expression Assay by Western Blot

Cells were washed twice with PBS (Life Technologies) and lysed in RIPA buffer (Sigma-Aldrich) containing 1% protease inhibitor cocktail (vol/vol, Sigma-Aldrich) on ice. Supernatants of cell lysates were obtained by centrifugation at 13,000 rpm for 15 minutes. Protein extracts were denatured by addition of sample buffer (Bio-rad) followed by boiling for 10 minutes, resolved by SDS-PAGE, and then transferred to PVDF membranes (Bio-rad). Subsequently, the membranes were blocked in Odyssey® Blocking buffer (Li-cor) and then incubated with GLUT5 or Actin primary antibodies. Primary antibodies were detected with fluorescent secondary antibodies (Li-cor).

Quantitative Real-time PCR (Q-PCR)

The expression of *SLCA2A5* was measured by Q-PCR. 18S rRNA was used as the internal control. The assay was conducted using Platinum® SYBR® Green qPCR SuperMix on a Roche Light Cycler® 480 Ⅱ PCR machine (Roche, Indianapolis, Indiana, US). The primers for human *SLCA2A5* were 5'-TCTGTAACCGTGTCCATGTTTC-3' (forward primer) and 5'-CATTAAGATCGCAGGCACGATA-3' (reverse primer). The primers for mouse *SLCA2A5* were 5'-TCTCTTCCAACGTGGTCCCTA -3' (forward primer) and 5'-GAGACTCCGAAGGCCAAACAG-3' (reverse primer). The primers for human 18S rRNA were 5'-CGGCGACGACCCATTCGAAC-3' (forward primer) and 5'- GAATCGAACCCTGATTCCCCGTC-3' (reverse primer). The primers for mouse 18S rRNA were 5'-GCAATTATTCCCCATGAACG-3' (forward primer) and 5'-GGCCTCACTAAACCATCCAA-3' (reverse primer).

Microarray Data and Gene Mutation Data Analysis

For the gene expression data sets including GSE 9476, GSE 37307, GSE 1159 and GSE 12417, raw data (CEL files) were

downloaded from the NCBI Gene Expression Omnibus (http://www.ncbi.nlm.nih.gov/geo/). These data were normalized using MAS 5.0 algorithm (Gautier et al., 2004) followed with $\log_2$ transformation. For the data set GSE 425, online normalized data were used directly. Kaplan-Meier survival analysis and meta-analysis were performed using Bioconductor package "survcomp" (Schroder et al., 2011). All the analyses were performed with the use of R (version 2.15.0, www.r-project.org) and Bioconductor packages (Gentleman et al., 2004). TCGA gene mutation data were downloaded from the Cancer Genome Atlas database (http://cancergenome.nih.gov/).

Colony Formation Assay in Soft Agar

The colony formation assay was performed as previously described with minor changes (Rivera et al., 2012). Briefly, cells were harvested and rinsed twice in PBS to completely remove residual media. Then, cells were seeded on 0.35% top agarose (Sigma-Aldrich) overlaided onto solidified 0.7% agarose in glucose-free RPMI 1640 containing 10% dFBS and additive sugar(s) as indicated in figures. Cultures were fed every week. Colonies were analyzed at the time point indicated in figures or figure legends.

Migration and Invasion Assay

AML cell migration was assessed in Corning Transwell Permeable Supports with polycarbonate membranes (24-well plate, 8 μm pore size). AML cells were harvested, rinsed twice in PBS, resuspended in glucose-free and serum-free RPMI 1640 containing sugar(s) as indicated in figures, and seeded into the upper chambers of the transwell plates at a density of 2×10^5/well. The lower chamber of each well was filled with complete medium containing 10% dFBS and sugar(s) as indicated in figures. After incubation of 16 hours, migrating U937 and OCI-AML3 cells were measured using the CCK-8 kit. The migrating K562 cells were detected using the protocol previously reported (Dutta et al., 2010).

Invasion assays were performed using the Corning Biocoat Martrigel Invasion Chamber (24-well plate, 8 μm pore size). The Matrigel was rehydrated prior to use by adding warm glucose-free RPMI 1640 to the interior of the insert. AML cells were resuspended in glucose-free and serum-free RPMI 1640 containing sugar(s) as indicated in figures, and seeded into the upper chambers at a density of 1×10^6/well. After incubation for 16 hours, invading U937 and OCI-AML3 cells were counted using the CCK-8 kit, while invading K562 cells were detected using the protocol previously reported (Dutta et al., 2010).

Supplemental References:

Bruckert, P., Kappler, R., Scherthan, H., Link, H., Hagmann, F., and Zankl, H. (2000). Double minutes and c-MYC amplification in acute myelogenous leukemia: Are they prognostic factors? Cancer genetics and cytogenetics *120*, 73-79.

Dutta, A., Sen, T., and Chatterjee, A. (2010). Culture of K562 human myeloid leukemia cells in presence of fibronectin expresses and secretes MMP-9 in serum-free culture medium. International journal of clinical and experimental pathology *3*, 288-302.

Gautier, L., Cope, L., Bolstad, B. M., and Irizarry, R. A. (2004). affy--analysis of Affymetrix GeneChip data at the probe level. Bioinformatics *20*, 307-315.

Gentleman, R. C., Carey, V. J., Bates, D. M., Bolstad, B., Dettling, M., Dudoit, S., Ellis, B., Gautier, L., Ge, Y., Gentry, J., *et al.* (2004). Bioconductor: open software development for computational biology and bioinformatics. Genome biology *5*, R80.

Keung, Y. K., Beaty, M., Powell, B. L., Molnar, I., Buss, D., and Pettenati, M. (2004). Philadelphia chromosome positive myelodysplastic syndrome and acute myeloid leukemia-retrospective study and review of literature. Leukemia research *28*, 579-586.

Lillington, D. M., Young, B. D., Berger, R., Martineau, M., Moorman, A. V., and Secker-Walker, L. M. (1998). The t(10;11)(p12;q23) translocation in acute leukaemia: a cytogenetic and clinical study of 20 patients. European 11q23 Workshop participants. Leukemia *12*, 801-804.

Lowenberg, B. (2008). Acute myeloid leukemia: the challenge of capturing disease variety. Hematology Am Soc Hematol Educ Program *2008*, 1-11.

Rivera, Z., Ferrone, S., Wang, X., Jube, S., Yang, H., Pass, H. I., Kanodia, S., Gaudino, G., and Carbone, M. (2012). CSPG4 as a target of antibody-based immunotherapy for malignant mesothelioma. Clin Cancer Res *18*, 5352-5363.

Schroder, M. S., Culhane, A. C., Quackenbush, J., and Haibe-Kains, B. (2011). survcomp: an R/Bioconductor package for performance assessment and comparison of survival models. Bioinformatics *27*, 3206-3208.